BIOIMAGING IN NEURODEGENERATION

BIOIMAGING IN NEURODEGENERATION

EDITED BY

PATRICIA A. BRODERICK, PhD

Department of Physiology and Pharmacology,
City University of New York Medical School;
Department of Neurology, New York University
School of Medicine; NYU Comprehensive
Epilepsy Center,New York, NY

DAVID N. RAHNI, PhD

Department of Chemistry and Physical Sciences
Pace University, Pleasantville, NY

EDWIN H. KOLODNY, MD

Department of Neurology
New York University School of Medicine
New York, NY

HUMANA PRESS
TOTOWA, NEW JERSEY

999 Riverview Drive, Suite 208
Totowa, New Jersey 07512

humanapress.com

For additional copies, pricing for bulk purchases, and/or information about other Humana titles, contact Humana at the above address or at any of the following numbers: Tel.: 973-256-1699; Fax: 973-256-8341; E-mail:humana@humanapr.com; Website: humanapress.com

Cover design by Patricia F. Cleary.

Cover illustrations: FOREGROUND, TOP: (*left*) Transaxial slice at the level of the striatum showing uptake of ^{99}m Tc-TRODAT-1 in dopamine transporters in a normal healthy volunteer; (*right*) a patient with hemi-PD exhibits a unilateral decrease in the uptake of ^{99}m Tc-TRODAT-1 in the side contralateral to clinical symptoms, most severely in the putamen (Chapter 2, Figs. 1 and 3; *see* full captions and discussion on p. 15.) FOREGROUND, MIDDLE: Regional NAA/Cr decrease in AD (Chapter 9, Fig. 2; *see* complete caption on p. 98 and discussion on p. 96). FOREGROUND, BOTTOM: Proton MRS (TE = 144 ms) in Canavan's disease demonstrating marked elevation in NAA caused by aspartoacylase deficiency (Chapter 21, Fig. 11; *see* full caption on p. 253 and discussion on p. 251). BACKGROUND: Hippocampal and entorhinal cortex boundary definition (Chapter 9, Fig. 1; *see* full caption on p. 97 and discussion on p. 96).

This publication is printed on acid-free paper. ∞

ANSI Z39.48-1984 (American National Standards Institute) Permanence of Paper for Printed Library Materials.

eISBN 1-59259-888-9

Printed in the United States of America. 10 9 8 7 6 5 4 3 2 1

Library of Congress Cataloging-in-Publication Data

Bioimaging in neurodegeneration / edited by Patricia A. Broderick, David N. Rahni, Edwin H. Kolodny.
p. cm.
Includes bibliographical references and index.
ISBN 1-58829-391-2 (alk. paper)
1. Brain--Degeneration--Imaging. I. Broderick, Patricia A., 1949- II. Rahni, David N. III. Kolodny, Edwin H.
RC394.D35B55 2005
616.8'04757--dc22

2004026624

Preface

Bioimaging is in the forefront of medicine for the diagnosis and treatment of neurodegenerative disease. Conventional magnetic resonance imaging (MRI) uses interactive external magnetic fields and resonant frequencies of protons from water molecules. However, newer sequences, such as magnetization-prepared rapid acquisition gradient echo (MPRAGE), are able to seek higher levels of anatomic resolution by allowing more rapid temporal imaging. Magnetic resonance spectroscopy (MRS) images metabolic changes, enabling underlying pathophysiologic dysfunction in neurodegeneration to be deciphered. Neurochemicals visible with proton ^{1}H MRS include *N*-acetyl aspartate (NAA), creatine/phosphocreatine (Cr), and choline (Cho); NAA is considered to act as an in vivo marker for neuronal loss and/or neuronal dysfunction. By extending imaging to the study of elements such as iron—elevated in several neurodegenerative diseases—laser microprobe studies have become extremely useful, followed by X-ray absorption fine-structure experiments.

Positron emission tomography (PET) and single-photon emission tomography (SPECT) have become important tools in the differential diagnosis of neurodegenerative diseases by allowing imaging of metabolism and cerebral blood flow. PET studies of cerebral glucose metabolism use the glucose analog [^{18}F] fluorodeoxyglucose analog ([^{18}F]FDG) and radioactive water ($H_2{}^{15}O$) and SPECT tracers use ^{99m}Tc-hexamethylpropylene amine oxime, (^{99m}Tc-HMPAO), and ^{99m}Tc-ethylcysteinate dimer (^{99m}Tc-ECD). Moreover, direct imaging of the nigrostriatal pathway with 6-[^{18}F]-fluoro-1-3,4-dihydroxyphenylalanine (FDOPA) in combination with PET technology, may be more effective at differentiating neurodegenerative diseases than PET or SPECT alone. Radioactive cocaine and the tropane analogs directly measure dopamine (DA) transporter binding sites and ^{99m}Tc-TRODAT-1 is a new tracer that could move imaging of the DA neuronal circuitry from the research environment to the clinic. [^{123}I] altropane SPECT may equal and further advance FDOPA PET.

Surgical treatments of neurodegenerative diseases are gaining attention as craniotomies become more routine, and as patients opt for surgery because they experience intractable responses to pharmacotherapy for neurodegeneration. These treatments fall into three categories: lesion ablation, deep brain stimulation (DBS), and restorative therapies such as nerve growth factor infusion or DA cell transplantation along the nigrostriatal pathway, particularly in Parkinson's disease. Also, electron micrographics image amyloid β aggregation in Alzheimer's disease (AD) and MRI (gadolinium enhanced) has been successfully exploited to image neuroinflammation in AD. MR-based volumetric imaging helps to predict the progression of AD via mild cognitive impairment (MCI) studies.

Novel neuroimaging technologies, such as neuromolecular imaging (NMI) with a series of newly developed BRODERICK PROBE® sensors, directly image neurotransmitters, precursors, and metabolites in vivo, in real time and within seconds, at separate and selective waveform potentials. NMI, which uses an electrochemical basis for detection, enables the differentiation of neurodegenerative diseases in patients who present with mesial versus neocortical temporal lobe epilepsy. In fact, NMI has some remarkable similarities to MRI insofar as there is technological dependence on electron and proton transfer, respectively, and further dependence is seen in both NMI and MRI on tissue composition such as lipids. NMI has already been joined with electrophysiological (EEG) and electromyographic (EMG) studies to enhance detection capabilities; the integration of NMI with MRI, PET, and SPECT can be envisioned as the next advance.

The tracer molecule, [^{11}C] α-methyl-L-tryptophan (AMT) is already used with PET to study serotonin (5-HT) deficiencies, presumably attributable to kynurenine enhancement in neocortical epilepsy patients. Moreover, AMT PET, in addition to FDG PET, provides reliable diagnosis for pediatric epilepsy syndromes such as West's syndrome. Important in children with cortical dysplasia (CD), FDG PET delineates areas of altered glucose, which can be missed by MRI. The new tracer, [^{11}C] flumazenil used with PET (FMZ PET), has found utility in the detection of epileptic foci in CD patients with partial epilepsies, and yet normal structural imaging is observed. Another new 5-HT1A tracer for PET imaging in abnormal dysplastic tissue is a carboxamide compound called [^{18}F]FCWAY.

Diagnosis of neocortical epilepsy has been significantly advanced by IOS or intrinsic optical signal imaging. IOS has its basis in the light absorption properties of electrophysiologically active neural tissue, activity caused by focal alterations in blood flow, oxygenation of hemoglobin, and scattering of light. IOS can map interictal spikes, onsets and offsets, and horizontal propagation lines. Thus, IOS is useful for diagnosing "spreading epileptiform depression." As with NMI, IOS holds promise for intraoperative cortical mapping wherein ictal and interictal margins can be more clearly defined. As does intraoperative MRI (iMRI) with neuronavigation, these technologies provide what is called "guided neurosurgery." Correlative imaging of general inhalational anesthetics such as nitrous oxide (N_2O) during intraoperative surgery is made possible by NMI technologies with nano- and microsensors.

NMI and MRI also enable the differential detection of white matter versus gray matter in discrete neuroanatomic substrates in brain, detection which is critical to both the epilepsies and the leukodystrophies. Although NMI is in its early stage in this arena, the immediate and distinct waveforms that distinguish white from gray matter are impressive. Moreover, the early finding of a leukodystrophy by MRI, particularly relevant for metachromatic leukodystrophy (MLD), Krabbe's disease (KD), and X-linked adrenoleukodystophy (ALD), allows clinicians therapeutic interventions before overt symptoms are exhibited. Imaging technologies, pathologies, clinical features, and treatments for these and other leukodystrophies, including peroxisomal disorders and leukodystrophies with macrocrania (Canavan's disease and Alexander's disease), are presented here in precise detail. The van der Knaap syndrome is a recently described leukodystrophy in vacuolating megaloencephalic leukoencephalopathy (VMI). This vanishing white matter disease highlights the potential of MRS imaging, which was used in its identification.

Bioimaging in Neurodegeneration provides extensive detail on pediatric mitochondrial disease, including imaging, pathologies, clinical features, and treatment or lack of treatment. It is extremely important to note that in pediatric mitochondrial cytopathies, a frequent finding on MRI is abnormal myelination, and infants with leukoencephalopathies, especially leukodystrophies, should be evaluated for mitochondrial cytopathy. Infarct-like, often transient lesions not confined to vascular territories are the imaging hallmark of mitochondrial myopathy, encephalopathy, lactic acidosis, and stroke-like episodes (MELAS). [^{31}P] MRS, which can measure transient changes in nonoxidative adenosine triphosphate (ATP) synthesis, and [^{1}H] MRS, which can measure lactate, are included in the mitochondrial imaging technologies.

Thus, *Bioimaging in Neurodegeneration* fulfills the current need to bring together neurodegeneration with bio- and neuroimaging technologies that actually enable diagnosis and treatment. Professionals in neurology, psychiatry, pharmacology, radiology, and surgery are among many who will greatly benefit. Neurodegenerative disease is divided into four areas, i.e., Parkinson's disease, Alzheimer's disease, the epilepsies, and the leukodystrophies. Chapter authors were selected for their formidable expertise in each field of medicine, their expertise in imaging technologies, and their scholarly contributions to medicine and science. Our appreciation is extended to them, and their staffs, for their fine research. We thank the editors and staff at Humana Press for their excellent assistance and support.

Patricia A. Broderick, PhD
David N. Rahni, PhD
Edwin H. Kolodny, MD

Contents

Contributors

PAUL D. ACTON, PhD • *Department of Radiology, University of Pennsylvania, Philadelphia, PA*

IMRAN I. ALI, MD • *Comprehensive Epilepsy Program, Medical College of Ohio, Toledo, OH*

SONYA BAHAR, PhD • *Department of Neurological Surgery, Weill Cornell Medical College, New York Presbyterian Hospital, New York, NY*

ANDREA BERNASCONI, MD • *Department of Neurology and Neurosurgery, McGill University, Montreal, QC, Canada*

ALBERTO BIZZI, MD • *Department of Neuroradiology, Instituto Nazionale Neurologico "C. Besta," Milan, Italy*

PATRICIA A. BRODERICK, PhD • *Department of Physiology and Pharmacology, City University of New York Medical School; Department of Neurology, New York University School of Medicine; NYU Comprehensive Epilepsy Center, New York, NY*

DIANE C. CHUGANI, PhD • *Department of Pediatrics, Wayne State University; PET Center, Children's Hospital of Michigan, Detroit, MI*

HARRY T. CHUGANI, MD • *Department of Pediatrics, Wayne State University; PET Center, Children's Hospital of Michigan, Detroit, MI*

VIJAY DHAWAN, PhD • *Center for Neurosciences, North Shore-Long Island Jewish Research Institute, New York University School of Medicine, Manhasset, NY*

RUDI A. DIERCKX, MD, PhD • *Department of Nuclear Medicine, University Hospital of Gent, Gent, Belgium*

MIRKO DIKSIC, PhD • *Department of Neurology and Neurosurgery, McGill University, Montreal, QC, Canada*

GLENN DRYHURST, PhD • *Department of Chemistry and Biochemistry, University of Oklahoma, Norman, OK*

DAVID EIDELBERG, MD • *Center for Neurosciences, North Shore-Long Island Jewish Research Institute, New York University School of Medicine, Manhasset, NY*

STANLEY FAHN, MD • *Department of Neurology, Columbia College of Physicians and Surgeons, New York, NY*

LAURA FARINA, MD • *Department of Neuroradiology, Instituto Nazionale Neurologico "C. Besta," Milan, Italy*

HUBERT H. FERNANDEZ, MD • *Department of Neurology, McKnight Brain Institute/University of Florida, Gainesville, FL*

CURT FREED, MD • *Neuroscience Center and Division of Clinical Pharmacology and Toxicology, University of Colorado Health Sciences Center, Denver, CO*

ANDREA L. GROPMAN, MD, FAAP, FACMG • *Division of Genetics and Metabolism, Departments of Pediatrics and Neurology, Georgetown University, Washington, DC*

DAVID R. HOWLETT, PhD • *Neurology & G.I. Centre of Excellence for Drug Discovery, GlaxoSmithKline, Harlow, Essex, UK*

CLIFFORD R. JACK, JR., MD • *Department of Radiology, Mayo Clinic, Rochester, MN*

BHARATHI DASAN JAGADEESAN, MD • *Department of Pediatrics, Wayne State University; PET Center, Children's Hospital of Michigan, Detroit, MI*

CSABA JUHÁSZ, MD, PhD • *Department of Pediatrics, Wayne State University; PET Center, Children's Hospital of Michigan, Detroit, MI*

KEJAL KANTARCI, MD • *Department of Radiology, Mayo Clinic, Rochester, MN*

GRAHAM J. KEMP, MA, DM, FRCPath, ILTM • *Division of Metabolic and Cellular Medicine, University of Liverpool, Liverpool, UK*

EDWIN H. KOLODNY, MD • *Department of Neurology, NYU School of Medicine, New York, NY*

JAKOB KORF, PhD • *Department of Biological Psychiatry, University Hospital of Groningen, Groningen, The Netherlands*

MENG LAW, MD, FRACR • *Department of Radiology, NYU Medical Center, New York, NY*

YILONG MA, PhD • *Center for Neurosciences, North Shore–Long Island Jewish Research Institute, New York University School of Medicine, Manhasset, NY*

W. R. WAYNE MARTIN, MD, FRCPC • *Movement Disorder Clinic, University of Alberta/Glenrose Rehabilitation Hospital, Edmonton, Alberta, Canada*

WAYNE MATSON PhD • *Systems Biology Section, Edith Nourse Rogers Memorial Veterans Hospital, VA New England Health Care System, Bedford, MA*

ASHESH MEHTA, MD, PhD • *Department of Neurological Surgery, Weill Cornell Medical College, New York Presbyterian Hospital, New York, NY*

JUN NATSUME, MD, PhD • *Department of Pediatrics, Japanese Red Cross Nagoya First Hospital, Nagoya, Aichi, Japan*

ANNETTE O. NUSBAUM, MD • *Department of Radiology, NYU School of Medicine, New York, NY*

STEVEN V. PACIA, MD • *Department of Neurology, NYU School of Medicine; NYU Comprehensive Epilepsy Center, New York, NY*

NOOR A. PIRZADA, MD • *Comprehensive Epilepsy Program, Medical College of Ohio, Toledo, OH*

DAVID N. RAHNI, PhD • *Department of Chemistry and Physical Sciences, Pace University, Pleasantville, NY*

STANLEY I. RAPOPORT, MD • *Brain Physiology and Metabolism Section, National Institute on Aging, National Institute on Health, Bethesda, MD*

PAULA D. RAVIN, MD • *Department of Neurology, University of Massachusetts Medical Center, Worcester, MA*

MARIO SAVOIARDO, MD • *Department of Neuroradiology, Instituto Nazionale Neurologico "C. Besta," Milan, Italy*

THEODORE H. SCHWARTZ, MD • *Department of Neurological Surgery, Weill Cornell Medical College, New York Presbyterian Hospital, New York, NY*

A. JON STOESSL, MD, FRCPC • *Pacific Parkinson's Research Centre, University of British Columbia, Vancouver, BC, Canada*

MINAH SUH, PhD • *Department of Neurological Surgery, Weill Cornell Medical College, New York Presbyterian Hospital, New York, NY*

ANDRÉ R. TROIANO, MD • *Pacific Parkinson's Research Centre, University of British Columbia, Vancouver, BC, Canada*

ADELINE VANDERVER, MD • *Child Neurology, Children's National Medical Center, Washington, DC*

JAN VERSIJPT, MD, PHD • *Department of Nuclear Medicine, University Hospital of Gent, Belgium; Department of Biological Psychiatry, University Hospital of Groningen, Groningen, The Netherlands*

LADISLAV VOLICER, MD, PhD • *Boston University School of Medicine and Edith Nourse Rogers Memorial Veterans Hospital, VA New England Health Care System, Bedford, MA*

EDWIN Y. WANG, MD • *Department of Radiology, NYU Medical Center, New York, NY*

DYLAN P. WINT, MD • *Department of Psychiatry, University of Florida/McKnight Brain Institute, Gainesville, FL*

MONIKA Z. WRONA, PhD • *Department of Chemistry and Biochemistry, University of Oklahoma, Norman, OK*

COMPANION CD

for *Bioimaging in Neurodegeneration*

Color versions of illustrations listed here may be found on the Companion CD attached to the inside back cover. The image files are organized into folders by chapter number and are viewable in most Web browsers. The number following "f" at the end of the file name identifies the corresponding figure in the text. The CD is compatible with both Mac and PC operating systems.

CHAPTER 2 FIGS. 1–5

CHAPTER 3 FIG. 2

CHAPTER 5 FIGS. 1, 4

CHAPTER 7 FIG. 1

CHAPTER 10 FIGS. 2, 3, AND 6

CHAPTER 11 FIG. 1

CHAPTER 14 FIGS. 1, 3, 6, 8, 9, 11–17

CHAPTER 15 FIGS. 1–5, 11

CHAPTER 16 FIGS. 2–5

Prologue

Nano- and Microimaging Surgical Anesthesia in Epilepsy Patients

PATRICIA A. BRODERICK, PhD, DAVID N. RAHNI, PhD, AND STEVEN V. PACIA, MD

Nitrous oxide (N_2O) is a simple and small molecule, consisting of two nitrogen atoms and one oxygen atom (Fig. 1). Yet, its anesthetic, analgesic, and psychotropic properties are indisputable *(1–3)*. Nitrous oxide is reported to act via opiate mechanisms because it induces met-enkephalin and β-endorphin release in rat and human, and the antinociceptic properties of nitrous oxide are reversible by naloxone *(4,5)*. Also, but likely not exclusively, nitrous oxide may exert its effects via glutamate receptors, that is, administration of (80%) nitrous oxide to rat hippocampus depresses excitatory currents evoked by *N*-methyl-D-aspartate *(6,7)*.

The combination of nitrous oxide and oxygen has found its way into prehospital emergency treatment of pain *(2)*. Under the proprietary names, Entonos® and Dolonox®, this combination in a 40–60% ratio is used by paramedics when treating acute myocardial infarction *(8)*. In some areas of the world, it is used in emergency medicine in lieu of opioid analgesics for the management of painful injuries *(9)*.

In the hospital setting, intraoperatively nitrous oxide is used adjunctly with other general anesthetics for its well-known "second gas effect," a phenomenon that is caused by its ability to diffuse quickly from alveoli. However, nitrous oxide, even in combination with oxygen, rarely is used alone in surgery because it is a relatively weak general anesthetic (low blood/gas solubility partition coefficient).

Interestingly, in studies used to map the effects of analgesics on pain, cerebral substrates for the nociceptive effects of nitrous oxide have been identified. Using low concentrations (20%) nitrous oxide was imaged using positron emission tomography and cerebral blood flow (rCBF). Inhalation of 20% nitrous oxide was found to be associated with enhanced rCBF in the anterior cingulate cortex (area 24), decreased rCBF in the hippocampus, posterior cingulate (areas 23,24), and decreased rCBF in the secondary visual cortices (areas 18,19; ref. *10*).

Despite the importance of this small and simple molecule in surgery, emergency medicine, and dentistry alone, there are virtually little or no direct techniques available to detect nitrous oxide unchanged in living tissue. Our purpose here is to present such a technique using neuromolecular imaging (NMI) and carbon based nano- and microsensors.

We describe the experimental design for and the results from in vitro assays, i.e., studies of nitrous oxide as N_2O is diffused into an electrochemical cell as well as those from in vivo assays, i.e., studies of nitrous oxide which has stabilized in living tissue from N_2O infusion.

This is the first report of the experimental assay for the gaseous solution, nitrous oxide and the results from such, in vitro. High purity (99.9%) commercially available nitrous oxide (T.W. Smith, Brooklyn, NY) was diffused using a flowmeter, calibrated at 10 psi, into an electrochemical cell containing saline/phosphate buffer for 5 min to allow the gas to reach saturation at room temperature. The flowmeter was purchased from Fisher Scientific (Bridgewater, NJ). Nitrous oxide concentrations in the approximate range of 10–100 μ*M* were achieved. Figure 2 shows a representative recording of nitrous oxide detection in vitro. Nitrous oxide detection occurred at the oxidation (half-wave) potential of 0.53 ± 0.02 V. In addition, DA and 5-HT signals are shown because increasing concentrations of DA and 5-HT were aliquoted into the electrochemical cell for use as standards. Thus, studies with the monoamines were conducted, which show the selective detection of nitrous oxide in the presence of the monoamine neurotransmitter.

Procedures for the detection of neurotransmitters and neurochemicals by BRODERICK PROBE® sensors are described *(11–20)*.

This is also the first report of the experimental assay for the gaseous solution, nitrous oxide, and the results from such, in vivo. Resected living tissue (hippocampal and neocortical) from temporal lobe epilepsy (TLE) patients was studied. Methods for patient classification and methods for delineating neurochemical profiles are previously published. Patients were administered nitrous oxide-oxygen anesthesia in a 40/60% concentration during intraoperative surgery. Figure 3 shows a representative recording from an NTLE patient, in vivo. These images from TLE patients show reliable nitrous oxide signals that occurred at the oxidation (half-wave) potential of 0.53 ±

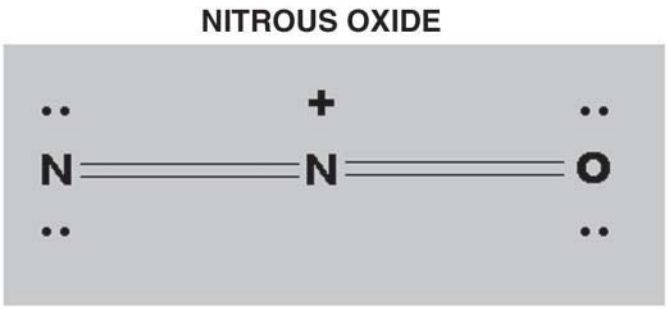

Fig. 1. The nitrous oxide molecule.

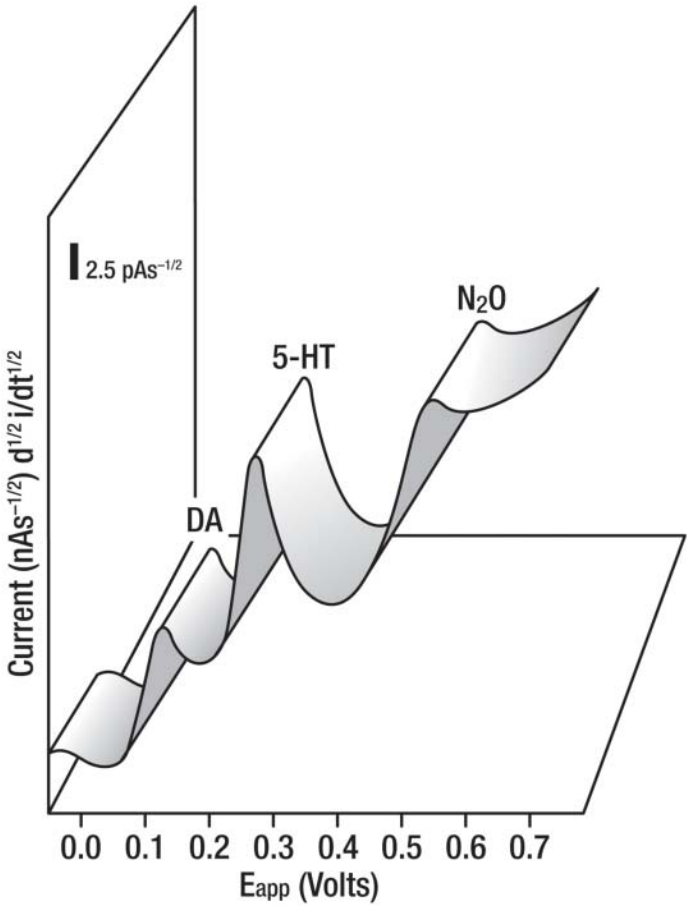

Fig. 2. A representative recording showing the detection of DA, 5-HT, and nitrous oxide (N_2O) in saline/phosphate buffer by the BRODERICK PROBE® stearate sensor in vitro. The oxidation (half-wave) potential for N_2O is 0.53 V ± 0.02 V. Oxidation potentials for monoamines confirm previous reports *(11–20)*. Note that the sensitivity of the sensor for the monoamine, 5-HT, is approximately two- to threefold greater than that for the monoamine DA as previously reported *(19)*.

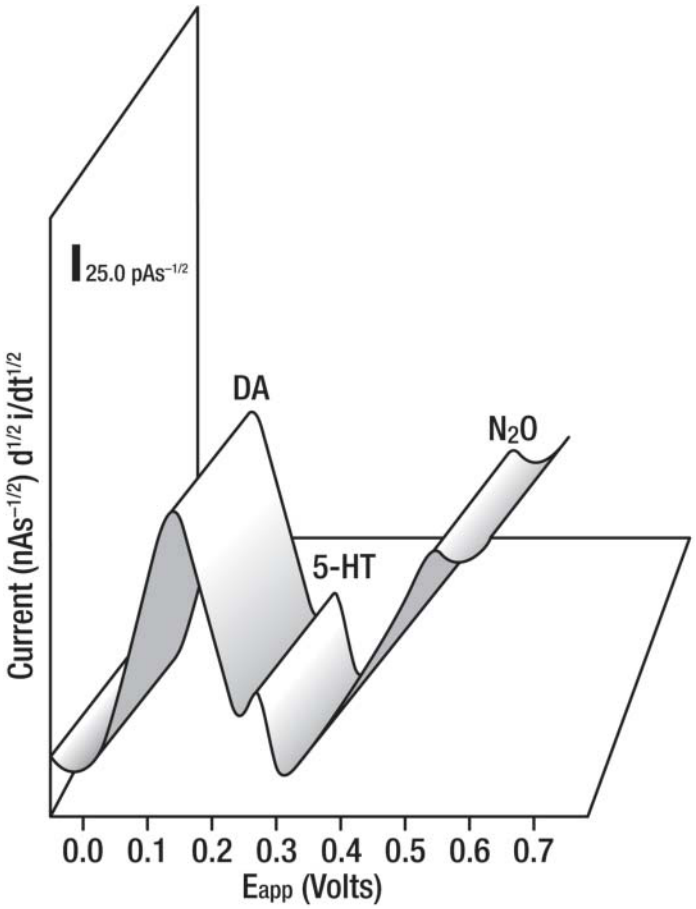

Fig. 3. A representative recording showing the detection of DA, 5-HT, and nitrous oxide (N_2O) in vivo in a TLE patient, specifically an NTLE patient, a subtype of TLE that typically exhibits DA and 5-HT; the study was performed with a BRODERICK PROBE® stearate sensor. The oxidation (half-wave) potential for N_2O is 0.53 V ± 0.02 V. Oxidation potentials for monoamines confirm previous reports *(11–18)*. Note that in vivo data exhibit greater concentrations for catecholamines than for indoleamines with the noted exception of white matter imaging *(20)*.

0.02 V, which is consistent with the detection of nitrous oxide at the same oxidation potential in vitro. Further evidence for the reliable detection of nitrous oxide comes from studies in this laboratory which has shown the separate detection of nitric oxide (NO) at an approximate oxidation potential of 0.75V *(21)*. These data are in general agreement with detection of NO using the carbon fiber electrode *(22)*. Moreover, the reliable detection of nitrous oxide comes from the known predictive ability to detect oxygen at early negative potentials, again separating the detection of oxygen from that of nitrous oxide. Finally, the stability of nitrous oxide at physiological temperatures is known (url: www.chm.bris.ac.uk/motm/n2o/n2oh.htm [*23;* retrieved on or about June 3, 2004]). Thus, these studies confirm the selective detection of nitrous oxide in the absence and presence of the monoamine neurotransmitters.

Table 1 shows the neuroanatomic location of nitrous oxide signals imaged in distinct neocortical neuroanatomic structures and hippocampal subparcellations. As expected, there was no

Table 1
Nitrous Oxide (N_2O) in Resected Temporal Tissues From Human Epilepsy Patients

Patient Number	*Epilepsy Type*	*N_2o Signals Imaged in:*	
2	MTLE	Neocortex (G)	
3	NTLE	Neocortex (G,W);	HPC (Granular cells)
4	NTLE	Neocortex (G,W);	HPC (Polymorphic layer)
5	MTLE	Neocortex (G)	
6	MTLE	HPC (Subiculum)	
8	MTLE	HPC (Pyramidal layer)	
9	NTLE	HPC (Pyramidal layer)	
10	NTLE	Neocortex (G)	
13	MTLE	Neocortex (G,W);	HPC (Polymorphic, Pyramidal, Mol. layers)
14	MTLE	Neocortex (G);	HPC (Subiculum)
15	MTLE	Neocortex (G,W);	HPC (Polymorphic layer)
16	MTLE	Neocortex (G,W)	

G is gray matter; W is white matter; Patients 7, 11, and 12: MTLE did not exhibit N_2O; NTLE, neocortical temporal lobe epilepsy; MTLE, mesial temporal lobe epilepsy.

apparent difference in the degree of nitrous oxide imaging between NTLE and MTLE patients, given the caveat that there were more MTLE patients than NTLE patients.

In summary, the significance of imaging nitrous oxide anesthesia in living tissue is paramount in neurology, neurosurgery, emergency medicine, toxicology, substance abuse (*see* ref. *24* for a recent review), and dentistry. Moreover, the BRODERICK PROBE® sensors image nitrous oxide signals on line yet separately from monoamines, metabolites, precursors, These data provide promise for optimizing such a technology for selective nano- and micromonitoring and measuring nitrous oxide intraoperatively.

ACKNOWLEDGMENTS

Protocol for human studies was approved by CUNY and NYU Investigational Review Boards. We thank the FACES Campaign, Parents Against Childhood Epilepsy (PACE Foundation), and the National Institute of Health, NIH/NIGMS SCORE AWARD # SO 6 GM 08168 for partial financial support. The authors gratefully acknowledge Bridget T. O'Sullivan, O.P., M.A., Msgr. Scanlan High School, and Karen Schulz, Humana Press, for secretarial and artistic assistance, respectively. We also thank Ratna Medicherla, CUNY medical student, for assistance with formula and table format.

REFERENCES

1. Archer WH. Life and letters of Horace Wells, discoverer of anesthesia. J Am Coll Dent 1944;11:81.
2. Thompson PL, Lown B. Nitrous oxide as an analgesic in acute myocardial infarction. J Am Med Assoc 1976;235:924.
3. Gillman MA. Nitrous oxide abuse in perspective. Clin Neuropharmacol 1992;15:297.
4. Zuniga JR, Joseph SA, Knigge KM. The effects of nitrous oxide on the central endogenous pro-opiomelanocortin system in the rat. Brain Res 1987;420:57–65.
5. Chapman CR, Benidetti C. Nitrous oxide effects on cerebral evoked potential to pain: Partial reversal with a narcotic antagonist. Anesthesiology 1979;51:135–138.
6. Mennerick S, Jevtovic-Todorovic V, Todorovic SM, Shen W, Olney JW, Zorumski CF. Effect of nitrous oxide on excitatory and inhibitory synaptic transmission in hippocampal cultures. J Neurosci 1998;18:9716–9726.
7. Jevtovic-Todorovic V, Todorovic SM, et al. Nitrous oxide (laughing gas) is an NMDA antagonist, neuroprotectant and neurotoxin. Nat Med 1998;4:460–463.
8. O'Leary U, Puglia C, Friching T D, Kowey PR. Nitrous oxide anesthesia in patients with ischemic chest discomfort: effect on beta-endorphins. J Clin Pharmacol 1987;27:957.
9. Malamed SF, Clark MS. Nitrous oxide-oxygen: a new look at a very old technique. J Calif Dent Assoc 2003;31:397–403.
10. Gyulai F, Firestone LL, Mintum M, Winter P. In Vivo Imaging of human limbic responses to nitrous oxide inhalation. Anesth Analg 1996;83:291–298.
11. Broderick PA, Pacia SV, Doyle WK, Devinsky O. Monoamine neurotransmitters in resected hippocampal subparcellations from neocortical and mesial temporal lobe epilepsy patients: in situ microvoltammetric studies. Brain Res 2000;878:49–63.
12. Pacia SV, Doyle WK, Broderick PA. Biogenic amines in the human neocortex in patients with neocortical and mesial temporal lobe epilepsy: identification with in situ micovoltammetry. Brain Res 2001;899:106–111.
13. Pacia SV, Broderick PA. Bioimaging L-tryptophan in human hippocampus and neocortex: subtyping temporal lobe epilepsy. In: Broderick PA, Rahni DN, Kolodny EH, editors. Bioimaging in Neurodegeneration, Totowa, NJ: Humana Press, 2005, pp. 141–147.
14. Broderick PA. Distinguishing in vitro electrochemical signatures for norepinephrine and dopamine. Neurosci Lett 1988;95:275–280.
15. Broderick PA. Characterizing stearate probes in vitro for the electrochemical detection of dopamine and serotonin. Brain Res 1989;495:115–121.
16. Broderick PA. Microelectrodes and their use in cathodic electrochemical arrangement with telemetric application. 1995; US Patent #5,433,710.1996; European Patent #90914306.7.

17. Broderick PA. Microelectrodes and their use in an electrochemical arrangement with telemetric application. 1999; US Patent #5,938,903.
18. Broderick, PA, Pacia SV. Identification, diagnosis and treatment of neuropathologies, neurotoxicities, tumors and brain and spinal cord injuries using microelectrodes with microvoltammetry. 2002;#PCT/USO2/11244. Pending 2002; US 10/118,571. Pending.
19. Broderick PA. Striatal neurochemistry of dynorphin-(1–13): In vivo electrochemical semidifferential analyses. Neuropeptides 1987;10: 369–386.
20. Broderick PA, Pacia SV. Imaging white matter signals in epilepsy patients: A unique sensor technology. In: Broderick PA, Rahni DN, Kolodny EH, editors. Bioimaging in Neurodegeneration, Totowa, NJ: Humana Press, 2005, pp. 199–206.
21. Rahni DN, Pacia SV, Broderick PA, A novel microvoltammetric approach for the determination of nitrous and nitric oxides: human epilepsy. Soc. Neurosci. Abstr. 2001, Orlando, Fl.
22. Crespi F, Campagnola M, Neudeck A, et al. Can voltammetry measure nitrogen monoxide (NO) and/or nitrites? J Neurosci Methods 2001;109(1):59–70.
23. Url: www.chm.bris.ac.uk/motm/n_2o/$n_2$oh.htm [retrieved on or about June 3rd, 2004]).
24. Bonson KR, Baggott M. Emerging drugs of abuse: use patterns and clinical toxicity. In: Massao EJ, Broderick PA, Mattson JL, Schardein JL, Schlaepfer TE, editors. Handbook of Neurotoxicology, Vol. 2, Totowa, NJ: Humana Press, 2002, pp. 223–257.

PARKINSON'S DISEASE

I

1 Magnetic Resonance Imaging and Magnetic Resonance Spectroscopy in Parkinson's Disease

Structural vs Functional Changes

W. R. WAYNE MARTIN, MD, FRCP

SUMMARY

At present, conventional magnetic resonance imaging (MRI) shows no convincing structural changes in Parkinson's disease (PD) itself, but it may be useful in helping to distinguish PD from other neurodegenerative parkinsonian syndromes. Magnetic resonance spectroscopy (MRS) also may provide useful information in distinguishing PD from disorders such as multiple system atrophy. The general field of MRI and MRS is evolving rapidly, and a number of new developments may provide relevant information. Novel pulse sequences, for instance, may provide more information regarding substantia nigra pathology in PD. The use of MR technologies to measure regional concentrations of brain iron should provide more information regarding the relationship between iron accumulation and parkinsonian symptoms. MRS provides a sensitive tool to investigate the possible contribution of abnormal brain energy metabolism to the pathogenesis of PD. MRS also allows the assessment of other metabolite changes in PD, for example, providing for the evaluation of associated changes in regional brain glutamate content. Last, functional MRI provides the potential to evaluate, in a noninvasive fashion, the role played by the basal ganglia in motor control and cognition in normal individuals as well as in PD.

Key Words: Parkinson's disease; T_2-weighted imaging; T2* effect; brain iron; substantia nigra imaging; progressive supranuclear palsy; hummingbird sign; multiple system atrophy; corticobasal degeneration; voxel-based morphometry; diffusion-weighted imaging; magnetic resonance spectroscopy; brain energy metabolism; mitochondrial function; ^{31}P-magnetic resonance spectroscopy; functional MRI; event-related fMRI.

From: *Bioimaging in Neurodegeneration*
Edited by P. A. Broderick, D. N. Rahni, and E. H. Kolodny

1. INTRODUCTION

The continuing evolution of new techniques for imaging the central nervous system has produced significant advances in the investigation of patients with neurodegenerative disorders and in our understanding of basal ganglia function. Although magnetic resonance imaging (MRI) has made possible the correlation of structural abnormalities identified in vivo with specific neurologic syndromes such as parkinsonism, changes in cerebral function do not always parallel changes in structure. Magnetic resonance spectroscopy (MRS) has provided insights into some of the underlying metabolic abnormalities, thereby providing further insights relating to the underlying pathophysiology of these neurodegenerative syndromes. Brain activation studies with functional MR imaging (fMRI) have provided additional information regarding the abnormalities in brain function associated with these disorders.

2. MRI IN PARKINSONISM

Conventional MRI is based primarily on the interplay between external magnetic fields and the resonant frequency of water protons in tissue. Image contrast is related to the specific imaging parameters used but typically represents a complex function of proton density and the longitudinal (spin-lattice) relaxation time (T_1) and transverse (spin–spin) relaxation time (T_2) of protons in tissue. Inhomogeneities in the magnetic field induced by tissue attributes also have an important effect on image contrast, termed T_2*. T_1-weighted images tend to display superior gray–white matter differentiation compared with T_2-weighted sequences, allowing a clear delineation, for example, of the head of the caudate nucleus from the lenticular nucleus and of the cerebral cortex from adjacent white matter. Newer sequences, such as magnetization-prepared rapid acquisition gradient echo (MPRAGE), allow for very short imaging times and high anatomical resolution. Volumetric studies using MPRAGE sequences with multiple thin slices are useful in studies that quantify tissue atrophy. On T_2-weighted images from high field strength MRI systems (1.5 T and greater), the lenticular nucleus is readily subdivided into the globus pallidus

and putamen, with the former structure displaying reduced signal intensity as compared with the latter. This differentiation is not present at birth but becomes evident within the first year or two of life, gradually increasing through the first three decades. The pallidal signal then remains relatively constant until the sixth or seventh decade, after which the signal attenuation becomes more prominent. Similar areas of reduced signal are also seen in the midbrain (red nucleus and substantia nigra pars reticulata), the dentate nucleus and, to a lesser extent, the putamen.

The prominent low-signal regions on T_2-weighted images correlate with sites of ferric iron accumulation as determined in vitro by Perls' Prussian blue stain *(1)*. Tissue iron produces a local inhomogeneity in the magnetic field that dephases proton spins, resulting in signal loss and decreased T_2 relaxation times (the T_2* effect). This iron susceptibility effect is best observed on heavily T_2-weighted images *(2,3)*. The T_2 changes are related to the strength of the static magnetic field and are not observed in normal individuals who are imaged with low field strength systems. It is important to note that gradient echo sequences are much more sensitive to iron-induced susceptibility changes than are the turbo spin echo (or fast spin echo) sequences that have become the routine method for producing T_2-weighted images on many clinical magnets.

In the early days of clinical MRI, the anatomical detail evident in images of the midbrain led investigators to evaluate this technology in patients with Parkinson's disease (PD), in whom the major neuropathological changes relate to neuronal loss from the midbrain substantia nigra pars compacta. As noted previously, T_2-weighted images show a prominent low signal area in the red nucleus and the substantia nigra pars reticulata, structures which are separated by the substantia nigra pars compacta. A narrowing, or smudging of this high signal zone separating the red nucleus and the pars reticulata has been reported in PD, consistent with the well-established pathological involvement in this area *(4,5)*. However, conventional MRI is not sufficiently sensitive at present to detect these changes in routine clinical applications. Although nigral changes in PD may be detected in population studies, technical factors, such as slice thickness, partial volume averaging, and head positioning, make it difficult to define reproducible abnormalities in individual patients in a structure as small as the substantia nigra. An alternative MRI approach to the study of midbrain pathology has been reported recently. This approach uses two inversion recovery pulse sequences, based on the hypothesis that contrast in T_1-weighted imaging depends mainly on the intracellular space and that T_1-weighted sequences are sensitive to the changes in intracellular volume that occur with cell death *(6)*. One sequence is designed to suppress peduncular white matter and the other to suppress nigral gray matter. These investigators reported structural changes in the nigra with this technique, even in the earliest cases of symptomatic disease. Hu et al.reported that structural changes in the nigra of patients with PD detected with inversion recovery sequences correlate with measures of striatal dopaminergic function using fluorodopa/positron emission tomography (PET; *7*).

Conventional MRI is of value in helping to differentiate PD from other neurodegenerative parkinsonian disorders. In progressive supranuclear palsy (PSP), MRI has been reported to delineate atrophy of the midbrain with a dilated cerebral aqueduct and enlarged perimesencephalic cisterns *(8)*. Patients with PSP have significantly decreased midbrain diameter than patients with PD and control subjects *(9)*. Atrophy of the rostral midbrain tegmentum produces the "hummingbird sign" on T_1-weighted midsagittal images, possibly corresponding to involvement of the rostral interstitial nucleus of the medial longitudinal fasciculus, a structure involved in the control of vertical eye movements *(10)*. Changes in the superior colliculus also may correlate with the eye findings, which are prominent in this condition *(11)*. Increased signal in periaqueductal regions also may be seen, coincident with the neuropathologic finding of gliosis in this region *(12)*. This technology is particularly valuable in the differential diagnosis of PSP, with up to 33% of patients with the typical clinical presentation having evidence of multiple cerebral infarcts on MRI *(13)*. Typical changes in a patient with PSP are illustrated in Fig. 1. In corticobasal degeneration, decreased signal intensity in the lenticular nucleus on T_2-weighted images, ventricular enlargement, and asymmetrical cortical atrophy has been reported *(14)*.

Imaging changes in multiple system atrophy (MSA), which help to differentiate this condition from PD, have been reported *(15–18)*. MSA typically is classified as a parkinsonian subtype (MSA-P), previously known as striatonigral degeneration (SND), and a cerebellar subtype (MSA-C), previously called olivopontocerebellar atrophy. The most widely reported change in MSA has been the presence, particularly on high field strength instruments, of a low signal in the putamen on T_2-weighted images. A "slit-like void" in the putamen on T_2-weighted images (and to a lesser degree on T_1-weighted images) in patients with SND has been reported, which Lang et al. *(19)* suggest is characteristic, if not pathognomonic, of this disorder. In this study, the MRI change correlated with the extent of neuronal loss and gliosis and with the pattern of iron deposition evident at autopsy. These authors and others *(20)* also reported a high signal rim on the lateral border of the putamen in SND on T_2-weighted images. Wakai et al. *(18)* reported in addition, atrophy in the putamen correlating with the severity of parkinsonian symptoms. Kraft et al. *(21)* have suggested that the combination of dorsolateral putamenal low-signal with a high-signal lateral rim is highly specific for MSA since it was found in 9 of their 15 MSA patients but in none of their 65 patients with PD and none of their 10 patients with PSP. In contrast, these authors found that putamenal low signal alone did not exclude a diagnosis of PD. A distinctive pontine high-signal abnormality, the "hot cross bun" sign, caused by a loss of pontine neurons and myelinated transverse pontocerebellar fibers with the preservation of the corticospinal tracts running craniocaudally, has been reported in patients with MSA *(22)*, although it is now clear that this appearance is not specific to this disorder *(23)*. Typical changes in a patient with suspected MSA-P are illustrated in Fig. 2. In olivopontocerebellar atrophy, MRI may show substantial atrophy of the cerebellar cortex and pons, accompanied by marked enlargement of the fourth ventricle *(24)*.

Schrag et al. *(25)* studied the specificity and sensitivity of routine MRI in differentiating atypical parkinsonian syn-

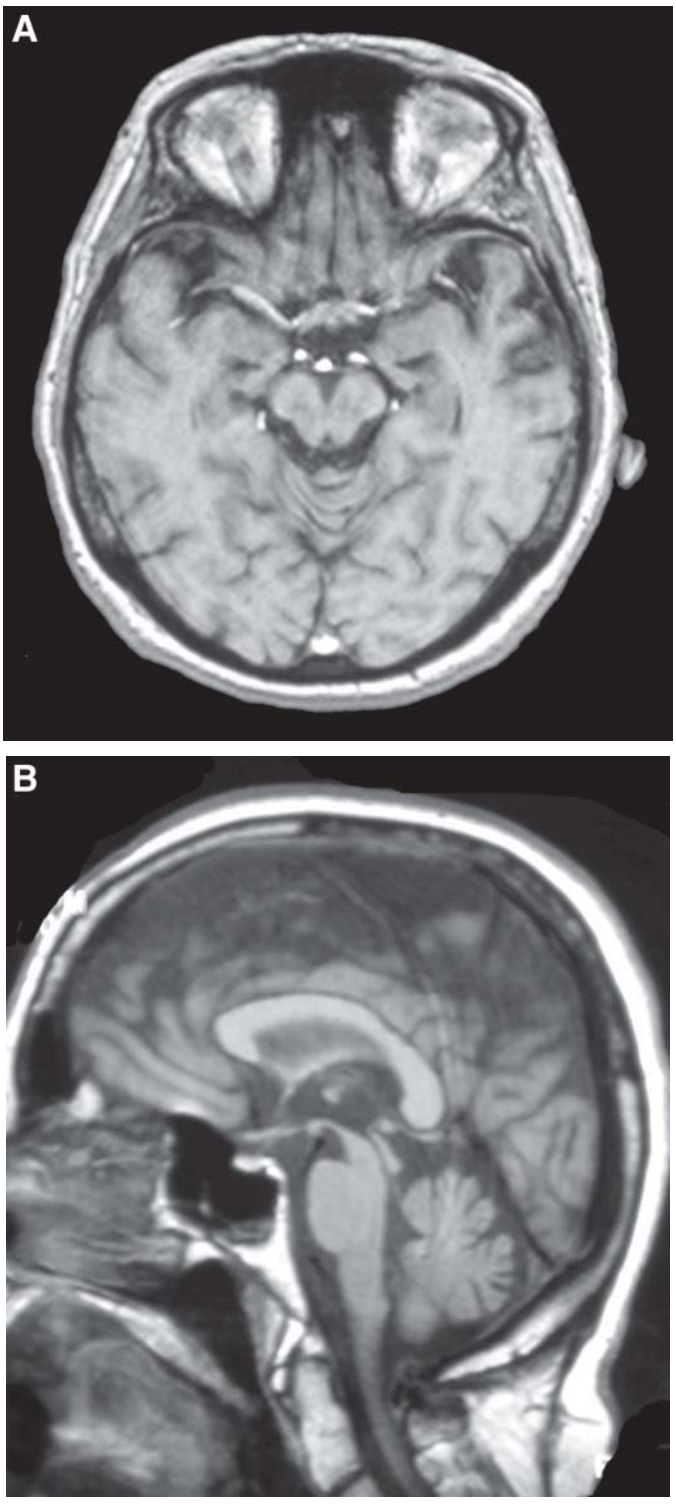

Fig. 1. Axial **(A)** and sagittal **(B)** images showing midbrain atrophy in PSP. Atrophy of the rostral midbrain tegmentum produces the "hummingbird sign" evident on the sagittal image.

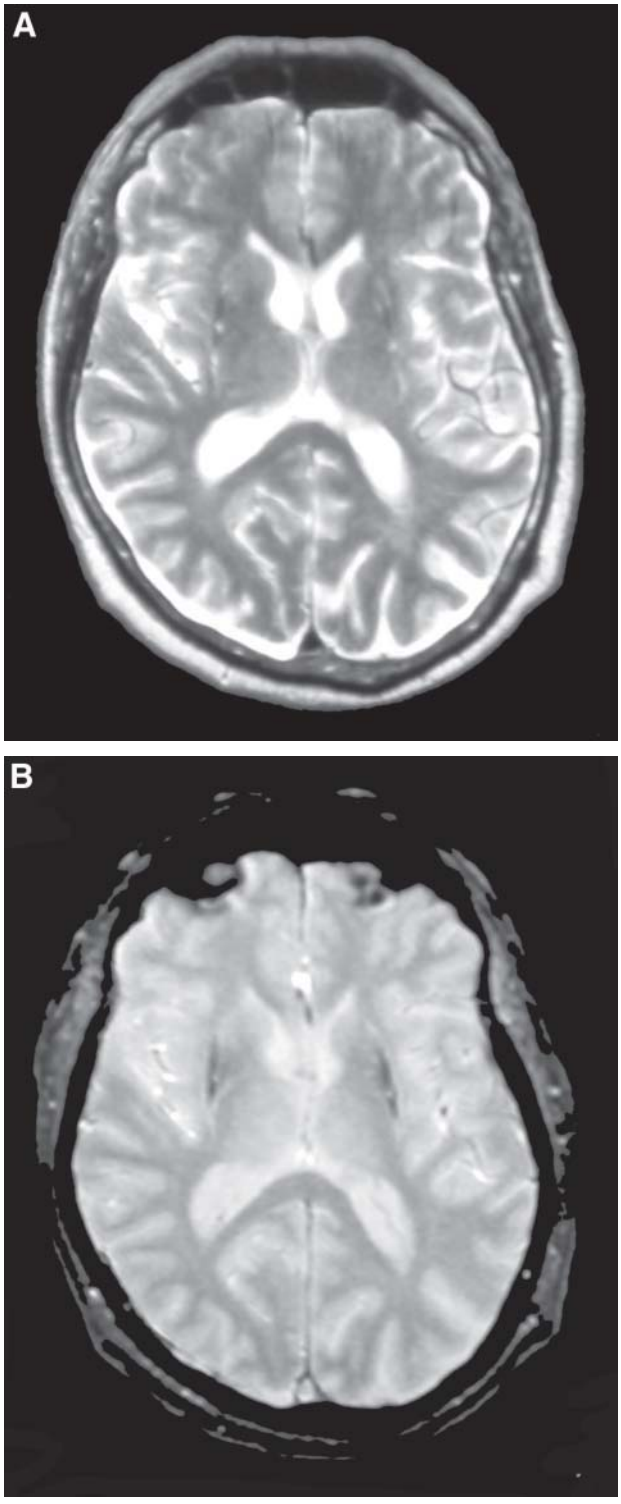

Fig. 2. Axial images of the striatum and midbrain in the parkinsonian subtype of MSA. T_2-weighted images **(A)** suggest a "slit-like" void with a high signal rim on the lateral border of the putamen, although the changes are subtle. Gradient echo images **(B)** show a more definite low-signal abnormality in the putamen. Pontine images (**C**, next page) show the "hot cross bun" sign.

dromes. In this report, more than 70% of patients with PSP and more than 80% of those with MSA-C could be classified correctly. In contrast, only approx 50% of patients with MSA-P could be classified correctly.

Three-dimensional volumetric measurements in PD, PSP, and MSA have demonstrated normal striatal, cerebellar, and brainstem volumes in PD but reduced mean striatal and

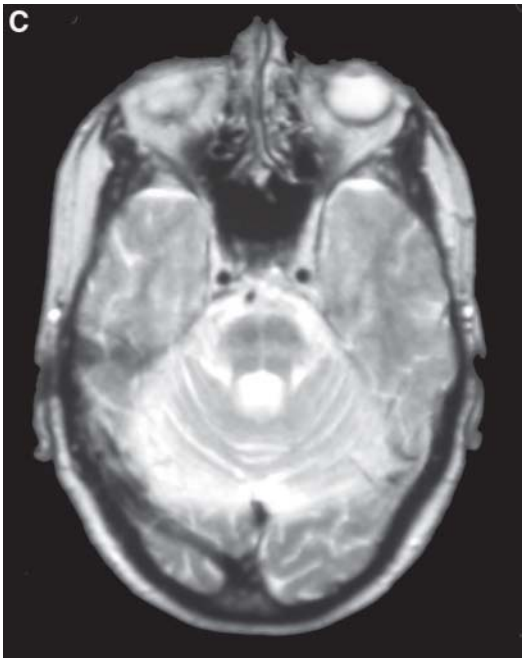

Fig. 2. (continued)

brainstem volumes in patients with MSA and PSP *(26)*. Those with MSA also showed a reduction in cerebellar volume. Although there was substantial overlap in volumetric measurements between groups, a discriminant analysis demonstrated effective discrimination of most of the MSA and PSP patients from the normal and PD groups. This analysis, however, did not separate PD patients from controls. The authors concluded that MRI-based volumetry might provide a marker to discriminate typical and atypical parkinsonism.

Voxel-based morphometry (VBM) recently has been applied to avoid the biases often associated with region of interest-guided volumetric measurements. VBM allows an objective, unbiased, comprehensive assessment of anatomical differences of gray and white matter throughout the brain, unconstrained by arbitrary region of interest selection. In MSA-P, VBM revealed selective cortical atrophy affecting primary and higher order motor areas, such as the supplementary motor area and anterior cingulate cortex *(27)*. Not surprisingly, VBM revealed a significant loss of cerebellar and brainstem volume in MSA-C *(28)*.

The analysis of serial MRI studies has been suggested *(29)* as a technique that is capable of demonstrating a characteristic pattern and progression of atrophy in a single patient with MSA in whom pathological confirmation of diagnosis was subsequently available. In this study, T_1-weighted volumetric scans acquired at two points 14 mo apart were analyzed using a previously validated nonlinear matching algorithm to obtain a voxel-by-voxel measure of volume change. The greatest rates of atrophy were reported in the pons, middle cerebellar peduncles, and the immediately adjacent midbrain and medulla.

Diffusion weighted imaging is a technique used to study the random movement of water molecules in the brain. Diffusion can be quantified by applying field gradients with varying degrees of diffusion sensitization, allowing the calculation of the apparent diffusion coefficient in tissue. Because the brain is organized in bundles of fiber tracts, water molecules move mainly along these structures, whereas diffusion perpendicular to the fiber tracts is restricted. Neuronal loss may alter the barriers restricting diffusion and increase the mobility of water molecules within the tissue architecture. In comparison with PD patients and control subjects, patients with MSA-P have been shown to have significantly higher apparent diffusion coefficient values in the putamen, with complete discrimination of MSA-P from PD based on these values *(30)*. Similar observations in comparison with controls have been reported in patients with PSP, although the results indicate that diffusion-weighted imaging does not differentiate PSP from MSA-P *(31)*.

As the above summary indicates, several different MRI techniques have been applied to these studies. Because of the variability in technique and the small number of patients included in most of these reports, further investigation is required to determine which MRI methodologies provide the highest sensitivity and specificity for the structural changes associated with PD and related neurodegenerative disorders. Although MRI may be of some benefit in differential diagnosis, it has not yet surpassed the role of the clinical neurologist in identifying these disorders.

MRI does play a major role, however, in the investigation of parkinsonism that may occur secondary to various structural brain lesions. Brain tumors may infiltrate or compress the basal ganglia and brainstem or, by vascular compression, may produce relative basal ganglia ischemia, thereby causing parkinsonism. Involvement of premotor frontal cortex by tumor may produce similar symptoms. Parkinsonism has been reported to occur in association with normal pressure or obstructive hydrocephalus, subdural hematoma, or multiple infarcts. MRI has a well-established role in the diagnosis of these disorders.

Focal basal ganglia lesions may also be demonstrated with MRI in some metabolic or toxic disorders associated with parkinsonism. Low-signal changes on all pulse sequences typically are present in basal ganglia calcification associated with idiopathic hypoparathyroidism or pseudohypoparathyroidism. Bilateral symmetrical necrosis of the globus pallidus may be evident in carbon monoxide *(32)* or cyanide poisoning *(33)* or multiple other toxic/metabolic disorders *(34)*.

3. QUANTITATIVE ESTIMATION OF REGIONAL BRAIN IRON WITH MRI

The adult brain has a very high iron content, particularly in the basal ganglia. Direct postmortem measurements have shown nonheme brain iron to be very low throughout the brain at birth but to increase gradually in most parts of the brain during the first two decades of life *(35)*. Brain iron concentration is maximal in the globus pallidus, substantia nigra, red nucleus, caudate, and putamen. Abnormally elevated iron levels are evident in various neurodegenerative disorders, including PD, in which increased iron in the substantia nigra has been reported *(36,37)*. Laser microprobe studies indicate that iron normally accumulates within neuromelanin granules of nigral

neurons and that iron levels within these granules are significantly increased in PD *(38)*. Extended X-ray absorption fine-structure experiments have shown that ferritin is the only storage protein detectable in both control and parkinsonian brain, with increased loading of ferritin with iron in PD *(39)*.

Although ferritin in aqueous solution has a strong effect on transverse relaxation times, these changes are much less prominent in tissue. Estimation of transverse relaxation times in patients with PD, using a 1.5-T whole-body imaging system, showed reduced T_2 values in substantia nigra, caudate, and putamen in PD patients as compared with healthy controls *(40)*. The decrease was small, however, and because of substantial overlap between groups, the investigators were unable to differentiate individual patients from controls with T_2 measurements. Vymazal et al. *(41)* reported nonsignificant T_2 shortening in the substantia nigra in PD consistent with iron accumulation. A more complex relationship between brain iron changes and disease state in PD, however, was suggested by Ryvlin et al. *(42)*. These authors reported decreased T_2 in the pars compacta of PD patients, regardless of disease duration, but increased T_2 values in the putamen and pallidum in those with duration of illness greater than 10 yr. In this study, putamen transverse relaxation time correlated positively with disease duration. Others have observed an imperfect correlation between T_2 values and quantitative assays of iron and ferritin *(43)*. The lack of a more substantial T_2 difference between PD and controls is not surprising because regional iron content is only one of several determinants of transverse relaxation times in tissue.

Several investigators have reported MR methods designed to estimate iron content directly. Bartzokis et al. used the influence of the strength of the external magnetic field on ferritin-induced T_2 changes to derive an index of regional tissue ferritin levels *(44)*. This method involves the measurement of transverse relaxation rates in the same patient with two different field strength instruments. Using this method, patients with earlier-onset PD (onset before the age of 60) were suggested to have increased ferritin in the substantia nigra, putamen, and globus pallidus, whereas later-onset patients had decreased ferritin in the substantia nigra reticulata *(45)*. Others have exploited the fact that paramagnetic substances, such as iron, create local magnetic field inhomogeneities that alter transverse relaxation times in the brain *(46,47)*. We have developed a method that quantifies the effects of paramagnetic centers sequestered inside cell membranes, based on the interecho time dependence of the decay of transverse magnetization caused by local field inhomogeneities that are the result of intracellular paramagnetic ions *(47)*. Because the concentration of brain iron is much greater than that of other paramagnetic ions, such as manganese and copper, this method enables the estimation of regional indices of brain iron content.

We used this technique to show a strong direct relationship between age and both putamen and caudate iron content *(48)*. This age-related increase may increase the probability of free-radical formation in the striatum, thereby representing a risk factor for the development of disorders such as PD in which nigrostriatal neurons may be affected by increased oxidant stress, although it should be noted that iron bound to ferritin might be relatively nonreactive and therefore unlikely to induce tissue damage. We also have reported a significant increase in iron content in the putamen and pallidum in PD and a correlation with the severity of clinical symptomatology with more severely affected patients having a higher iron content in these structures *(49)*. We have applied this methodology in striatonigral degeneration and have shown an increase in putamen iron content in this disorder, beyond the 95% confidence limit for inclusion in the PD group, even when considering severity of clinical symptomatology *(50)*. Our observations are summarized in Fig. 3. Using an alternate method developed by Ordidge and colleagues *(46)*, Gorell et al. reported an increase in iron-related MR contrast in the substantia nigra in PD, with a correlation between the increase and disease severity as indicated by simple reaction time *(51)*. Changes compatible with increased nigral iron content also have been reported by Graham et al. using a partially refocused interleaved multiple echo pulse sequence at 1.5 T, although these investigators suggested reduced iron content in the putamen *(52)*.

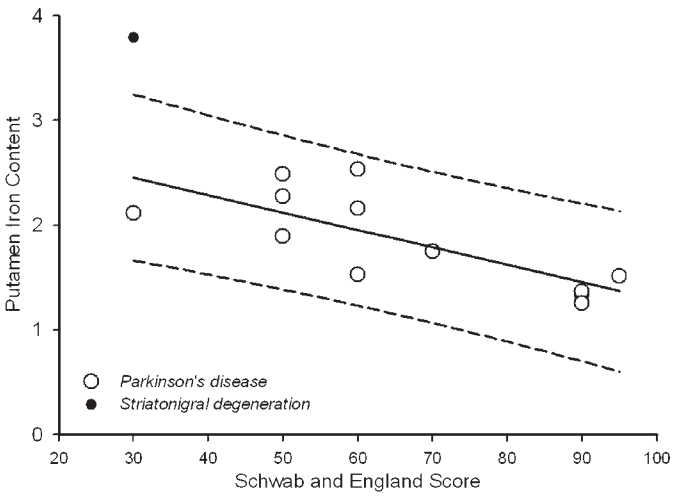

Fig. 3. Putamen iron content in PD and a patient with clinical diagnosis of the parkinsonian subtype of multiple system atrophy, expressed as a function of disease severity based on the Schwab and England activities of daily living score. The regression line and 95% confidence limits for inclusion in the PD group are indicated.

In summary, the application of MRI methods to study regional brain iron content is in its infancy. Much further investigation is required to determine which techniques are best able to provide quantifiable images that correspond to independent measures of brain iron and to determine the sensitivity and specificity of changes in basal ganglia iron content that might be associated with PD and other neurodegenerative disorders.

4. MRS IN PARKINSONISM

MRS provides a noninvasive method of quantifying the concentration of MR-visible metabolites in the brain. The technique is based on the general principle that the resonant frequency of a specific metabolite depends on its chemical

environment. Most clinical MRS studies have concentrated on the metabolites visible with proton (^{1}H) spectroscopy and measured in single, localized tissue volumes in the brain. The metabolites of interest that can be most readily studied with ^{1}H-MRS at long echo times include *N*-acetyl aspartate (NAA), creatine/phosphocreatine (Cr), and choline (Cho). Altered neuronal membrane synthesis and degradation can produce changes in Cho *(53)*. NAA is contained almost exclusively within neurons *(54)* and is therefore considered to act as an in vivo marker of neuronal loss or dysfunction. Reduced regional NAA concentration has been reported in conditions characterized by neuronal or axonal loss *(55–59)*. Most frequently, NAA measurements have been based on the regional NAA/Cr ratio. The rationale for the use of the Cr resonance as the denominator is based on the concept that creatine and phosphocreatine are in chemical equilibrium and that the total concentration of both compounds is expected to remain unchanged by neurodegenerative disease processes. Alternate methods are now available for the measurement of metabolite concentrations, such as those using water as an internal standard for calibration *(60)* and those involving calibration to an external standard *(61)*, which should allow for a significant improvement of the quantitative accuracy of ^{1}H-MRS.

Several studies that used ^{1}H-MRS in PD have been reported, reviewed by Davie *(62)* and systematically by Clarke and Lowry *(63)*. A large multicenter study of 151 patients with PD showed no significant difference in either NAA/Cr or NAA/Cho ratios between controls and patients who were not taking levodopa *(64)*. Other groups *(65–67)* have reported similar results. Similarly, in a small study using absolute metabolite quantitation, NAA, Cr, and Cho concentrations in PD did not differ significantly from those in controls *(68)*. Although no significant difference was observed in the NAA/Cr ratio in levodopa-treated patients with PD, Ellis et al. reported reduced NAA/Cr in drug-naïve PD patients compared with both the treated PD group and with the control group *(69)*. These authors suggested that the reduced ratio in PD might reflect a functional abnormality of neurons in the putamen that can be reversed with levodopa treatment. Clarke and Lowry have reported a significant decrease in the NAA/Cho ratio in PD because of an increase in the absolute concentration of Cho unassociated with a change in NAA concentration *(70)*.

O'Neill et al. have recently reported a small study using quantitative ^{1}H-MRS in which multiple tissue volumes were assessed *(71)*. This study applied more rigorous MR methodology than previous studies, including tissue segmentation to correct for varying gray and white matter content within the voxel of interest in different patients and the use of spectroscopic imaging to provide more widespread sampling of multiple brain regions. Observations from this study included decreased Cr concentration in the substantia nigra but normal NAA and Cho levels, suggesting that the use of simple ratios such as NAA/Cr may be misleading in PD. No differences in NAA, Cr, or Cho content were observed between PD patients and controls in either basal ganglia or multiple cortical volumes. This study also reported that the volumes of putamen, globus pallidus, and prefrontal cortical gray matter were significantly reduced in PD vs. age-matched controls. A negative correlation was observed between the volume of the substantia nigra pars compacta and that of the other basal ganglia nuclei in controls but not PD, although the volume measurements were based on MRI sequences yielding a relatively low spatial resolution. Cortical changes in PD have also been reported with a reduced NAA/Cr ratio in motor cortex *(72)* and in temporoparietal cortex *(73)*, possibly related to impaired neuronal function resulting from a loss of thalamocortical excitatory input.

In contrast to the apparent lack of changes in PD with MR spectroscopy, there does appear to be a significant reduction in basal ganglia NAA concentration in MSA. Davie reported ^{1}H-MRS studies in the lentiform nucleus in controls and in patients with PD and with clinically probable MSA *(65)*. In MSA, there was a significant reduction in absolute levels of NAA, particularly in patients with the SND subtype of MSA, suggesting that the spectroscopic measurement of NAA levels in the lentiform nucleus may provide a clinically useful technique to help differentiate MSA from PD. Federico et al. showed similar changes in MSA *(74)*. However, in a study using absolute quantitation of metabolite concentrations, NAA was reported to be unchanged in MSA *(70)*.

Axelson et al. have reported an alternate approach to the analysis of spectroscopic data based on pattern recognition utilizing an artificial neural network *(75)*. Conventional data analysis in this study showed no significant abnormalities in metabolite ratios in PD, whereas trained neural networks could distinguish control from PD spectra with considerable accuracy.

Several additional issues contribute to the variability of the results observed in these spectroscopic studies. Most of the studies reported only a small number of patients, often with fewer than 10 patients in each group. The patient groups themselves have varied somewhat from study to study, with some patients having early, untreated PD, and others having more advanced disease that requires treatment. Variabilities in the MR technique itself, for example, in the choice of echo time, may lead to heterogeneous results. Lastly, the high iron content in the basal ganglia has a significant impact on the ability to obtain reproducible high-resolution spectra from this region and may impact on the accuracy of quantitative results extracted from the spectra.

5. ENERGY METABOLISM IN PD

Although the etiology of PD is unknown, the possibility of an underlying defect in mitochondrial metabolism has been addressed in several biochemical studies *(76)*. There is evidence of reduced complex I activity in the substantia nigra in PD, and Gu et al. have suggested that a mitochondrial DNA abnormality may underlie this complex I defect in at least a subgroup of PD patients *(77)*. Studies in other tissues, however, have produced conflicting results, perhaps in part because biochemical studies involve removal of mitochondria from their natural milieu, with consequent mechanical disruption and a loss of normal control mechanisms. In contrast, MRS provides the potential to study mitochondrial metabolism in vivo.

The rate of intracellular energy metabolism is reflected by the ratio of inorganic phosphate (Pi) to phosphocreatine (PCr), readily measured with ^{31}P-MRS. The measurement of this ratio in resting muscle has been shown to be a useful diagnostic test

for mitochondrial disease *(78)*. Penn et al. have used ^{31}P-MRS to investigate energy metabolism in muscle in patients with PD. The Pi/PCr ratio was significantly increased in PD, suggesting a small, generalized mitochondrial defect *(79)*. Further studies are needed to determine whether these changes are limited to a clinically definable subset of parkinsonian individuals. ^{31}P-MRS studies of brain have recently been reported in MSA and PD *(80)*. In these studies, patients with MSA showed significantly increased Pi content and reduced PCr content, whereas those with PD showed significantly increased Pi but unchanged PCr, suggesting abnormal energy metabolism in both disorders.

The combination of ^{31}P-MRS and fluorodeoxyglucose/PET has been used to suggest that temporoparietal cortical glycolytic and oxidative metabolism are both impaired in nondemented PD patients *(81)*. These observations are consistent with a previous report of temporoparietal cortical reduction in NAA/Cr ratio in nondemented PD patients, which correlated with measures of global cognitive decline independently of motor impairment *(73)*.

An alternate approach to study energy metabolism is with ^{1}H-MRS. Normal brain energy production is derived from the oxidative metabolism of glucose by way of the Krebs cycle and, ultimately, the electron transport chain. A defect at the level of either of the two latter processes will result in decreased metabolism of pyruvate through these pathways, and increased production of lactate. Regional brain lactate concentrations can be readily assessed with ^{1}H-MRS. For example, this methodology has been used to demonstrate increased occipital lactate levels, thereby suggesting impaired energy metabolism in Huntington's disease *(82)*. We have found similar changes in some but not all patients with PD (W. R. W. Martin, unpublished observations), providing further evidence for the presence of a mitochondrial defect in this disorder. In contrast, however, Hoang et al. *(83)* have reported normal energy metabolism in the putamen and in occipital and parietal lobes when using both ^{31}P- and ^{1}H-MRS in patients with PD.

6. FUNCTIONAL MRI IN PD

Motor activation studies provide a means to investigate the regional cerebral mechanisms involved in motor control in normal subjects and in patients with disorders affecting these control systems. Typical fMRI experiments involve measurement of regional blood oxygen level-dependent signal increases associated with specific activation paradigms. These signal changes occur as a result of the increased local cerebral blood flow and altered oxyhemoglobin concentration associated with neuronal activation. Functional MRI experiments have extended our knowledge of disordered motor control systems, based on the extensive previous experience obtained with PET/motor activation studies in control subjects and in patients with PD. PET studies have suggested that cortical motor areas, such as the supplementary motor area (SMA), seem to be underactive in akinetic parkinsonian patients *(84,85)*, whereas other motor areas, such as the parietal and lateral premotor cortex and the cerebellum, appear to be overactive *(86)*. In comparison with PET, the application of MR-based methodology has allowed for improvements in both spatial and temporal resolution in activation studies.

Sabatini et al. *(87)* compared the changes induced by a complex sequential motor task performed with the right hand in six PD patients in the "off" state to six normal subjects. In control subjects, significant activation was seen in the left primary sensorimotor cortex, the left lateral premotor cortex, bilateral parietal cortex, the anterior cingulate cortex, and in the rostral and caudal parts of the supplementary motor area SMA. In PD patients, significant activation was seen bilaterally in primary sensorimotor cortex (left more than right), in bilateral parietal cortex, in cingulate cortex, and in the caudal but not the rostral SMA. Between-group comparisons showed increased activation of the rostral SMA and the right dorsolateral prefrontal cortex in controls, and increased activation of primary sensorimotor cortex, premotor cortex, and parietal cortex bilaterally, as well as the cingulate cortex, and the caudal SMA in PD. The decreased rostral SMA activation in PD is consistent with previous PET studies *(84,85)* and is thought to reflect a decrease in the positive efferent feedback from the basal ganglia-thalamocortical motor loop due to striatal dopamine depletion. The widespread increased activation in other motor areas also is consistent with previous PET studies *(86)* and suggests an attempt to recruit parallel motor circuits to overcome the functional deficit of the striatocortical motor loops. The high resolution of fMRI allowed the SMA to be subdivided into two functionally distinct areas in this study with the rostral component corresponding best to the decreased activation noted on previous PET studies *(87)*.

Event-related fMRI directly reflects signal changes associated with single movements, thereby avoiding the problem of a prolonged acquisition time, which may confound data by invoking cerebral processes unrelated to movement. Haslinger et al. *(88)* used this technique to study cerebral activation associated with single joystick movements in controls and in PD patients, both in the akinetic "off" state, and again in the "on" state after taking levodopa. Control subjects activated primary sensorimotor and adjoining cortex, as well as the rostral SMA. Patients in the "off" state showed significant underactivity in rostral SMA, as well as increased activation in primary motor and lateral premotor cortex bilaterally. These results are similar to those reported in the previous block design fMRI study described by Sabatini et al. *(87)*. In the "on" state, there was relative normalization of the impaired activation in the rostral SMA and of the increased activation in primary motor and premotor cortices. This event-related study provides an example of the exquisite sensitivity that can be achieved with fMRI, sufficient to demonstrate the metabolic/hemodynamic changes associated with the neuronal activity involved in generating a single voluntary movement.

7. SUMMARY AND CONCLUSIONS

At present, conventional MRI shows no convincing structural changes in PD itself, but it may be useful in helping to distinguish PD from other neurodegenerative parkinsonian syndromes and from the occasional case of parkinsonism secondary to a focal brain lesion. MRS also may provide useful information in distinguishing PD from disorders such as MSA.

The general field of MRI and MRS is evolving rapidly, and there are a number of areas in which we can expect new devel-

opments to provide relevant information. Novel pulse sequences may provide more information regarding substantia nigra pathology in PD. The use of MR as a tool to measure regional iron concentrations should provide more information regarding the relationship between iron accumulation and parkinsonian symptoms. MRS provides a sensitive tool for the researcher to investigate in vivo the possible contribution of abnormalities in brain energy metabolism to the pathogenesis of PD. MRS also allows the assessment of other metabolite changes in PD, for example, providing for the evaluation of the potential importance of changes in regional brain glutamate content. Lastly, fMRI provides the potential to evaluate, in a noninvasive fashion, the role played by the basal ganglia in motor control and in cognition in normal individuals as well as in PD.

REFERENCES

1. Rutledge JN, Hilal SK, Schallert T, Silver AJ, Defendini RD, Fahn S. Magnetic resonance imaging of Parkinsonisms. In: Fahn S, Marsden CD, Calne D, Goldstein M, editors. Recent Developments in Parkinson's Disease. Florham Park, NJ: Macmillan; 1987:123–134.
2. Olanow CW. Magnetic resonance imaging in parkinsonism. Neurol Clin 1992;10::405–420.
3. Rutledge JN, Hilal SK, Silver AJ, et al. Study of movement disorders brain iron by MR. AJNR Am J Neuroradiol 1987;8:397–411.
4. Duguid JR, De la Paz R, DeGroot J. Magnetic resonance imaging of the midbrain in Parkinson's disease. Ann Neurol 1986;20:744–747.
5. Braffman BH, Grossman RI, Goldberg HI, et al. MR imaging of Parkinson disease with spin-echo gradient-echo sequences. AJR Am J Roentgenol 1989;152:159–165.
6. Hutchinson M, Raff U. Structural changes of the subsantia nigra in Parkinson's disease as revealed by MR imaging. AJNR Am J Neurorad 2000;21:697–701.
7. Hu M.T.M., White SJ, Herlihy AH, et al. A comparison of 18F-dopa PET inversion recovery MRI in the diagnosis of Parkinson's disease. Neurology 2001;56:1195–1200.
8. Savoiardo M, Strada L, Girotti F, et al. MR imaging in progressive supranuclear palsy Shy-Drager syndrome. J Comput Assist Tomogr 1989;13:555–560.
9. Warmuth-Metz M, Naumann M, Csoti I, Solymosi L. Measurement of the midbrain diameter on routine magnetic resonance imaging. Arch Neurol 2001;58:1076–1079.
10. Kato N, Arai K, Hattori T. Study of the rostral midbrain atrophy in progressive supranuclear palsy. J Neurol Sci 2003;210:57–60.
11. Savoiardo M, Girotti F, Strada L, Ciceri E. Magnetic resonance imaging in progressive supranuclear palsy other parkinsonian disorders. J Neural Transm Suppl 1994;42:93–110.
12. Yagishita A, Oda M. Progressive supranuclear palsy: MRI pathological findings. Neuroradiology 1996;38:(Suppl 1):S60–S66.
13. Dubinsky RM, Jankovic J. Progressive supranuclear palsy a multi-infarct state. Neurology 1987;37:570–576.
14. Hauser RA, Olanow CW, Gold M, et al. Magnetic resonance imaging of corticobasal degeneration. J Neuroimaging 1996;6:222–226.
15. Drayer BP, Olanow W, Burger P, et al. Parkinson plus syndrome: diagnosis using high field MR imaging of brain iron. Radiology 1986;159:493–498.
16. Stern MB, Braffman BH, Skolnick BE, Hurtig HI, Grossman RI. Magnetic resonance imaging in Parkinson's disease parkinsonian syndromes. Neurology 1989;39:1524–1526.
17. Pastakia B, Polinsky R, Di Chiro G, Simmons JT, Brown R, Wener L. Multiple system atrophy (Shy-Drager syndrome): MR imaging. Radiology 1986;159:499–502.
18. Wakai M, Kume A, Takahashi A, Ando T, Hashizume Y. A study of parkinsonism in multiple system atrophy: clinical MRI correlation. Acta Neurol Scand 1994;90:225–231.
19. Lang AE, Curran T, Provias J, Bergeron C. Striatonigral degeneration: iron deposition in putamen correlates with the slit-like void signal of magnetic resonance imaging. Can J Neurol Sci 1994;21:311–318.
20. Konagaya M, Konagaya Y, Iida M. Clinical magnetic resonance imaging study of extrapyramidal symptoms in multiple system atrophy. J Neurol Neurosurg Psychiatry 1994;57:1528–1531.
21. Kraft E, Schwarz J, Trenkwalder C, Vogl T, Pfluger T, Oertel, WH. The combination of hypointense hyperintense signal changes on T2-weighted magnetic resonance imaging sequences: a specific marker of multiple system atrophy? Arch Neurol 1999;56:225–228.
22. Schrag A, Kingsley D, Phatouros C, et al. Clinical usefulness of magnetic resonance imaging in multiple system atrophy. J Neurol Neurosurg Psychiatry 1998;65:65–71.
23. Muqit MMK, Mort D, Miszkiel KA, Shakir RA. "Hot cross bun" sign in a patient with parkinsonism secondary to presumed vasculitis. J Neurol Neurosurg Psychiatry 2001;71:565–566.
24. Savoiardo M, Strada L, Girotti F, et al. Olivopontocerebellar atrophy: MR diagnosis relationship to multiple system atrophy. Radiology 1990;174:693–696.
25. Schrag A, Good CD, Miszkiel K, et al. Differentiation of atypical parkinsonian syndromes with routine MRI. Neurology 2000;54:697–702.
26. Schulz JB, Skalej M, Wedekind D, et al. Magnetic resonance imaging-based volumetry differentiates idiopathic Parkinson's syndrome from multiple system atrophy progressive supranuclear palsy. Ann Neurol 1999;45:65–74.
27. Brenneis C, Seppi K, Schocke MF, et al. Voxel-based morphometry detects cortical atrophy in the Parkinson variant of multiple system atrophy. Mov Disord 2003;18:1132–1138.
28. Specht K, Minnerop M, Abele M, Reul J, Wullner U, Klockgether T. In vivo voxel-based morphometry in multiple system atrophy of the cerebellar type. Arch Neurol 2003;60:1431–1435.
29. Schott JMM, Simon JE, Fox NC, et al. Delineating the sites progression of in vivo atrophy in multiple system atrophy using fluid-registered MRI. Mov Disord 2003;18:955–958.
30. Schocke MFH, Seppi K, Esterhammer R, et al. Diffusion-weighted MRI differentiates the Parkinson variant of multiple system atrophy from PD. Neurology 2002;58:575–580.
31. Seppi K, Schocke MFH, Esterhammer R, et al. Diffusion-weighted imaging discriminates progressive supranuclear palsy from PD, but not from the Parkinson variant of multiple system atrophy. Neurology 2003;60:922–927.
32. Davis PL. The magnetic resonance imaging appearances of basal ganglia lesions in carbon monoxide poisoning. Magn Reson Imaging 1986;4:489–490.
33. Rosenberg NL, Myers JA, Martin WRW. Cyanide-induced parkinsonism: clinical, MRI 6-fluorodopa positron emission tomography studies. Neurology 1989;39:142-144.
34. Marsden CD, Lang AE, Quinn NP, et al. Familial dystonia visual failure with striatal CT lucencies. J Neurol Neurosurg Psychiatry 1986;49:500–509.
35. Hallgren B, Sourander P. The effect of age on the nonhaemin iron in the human brain. J Neurochem 1958;3:41–51.
36. Dexter DT, Wells FR, Lees AJ, et al. Increased nigral iron content alterations in other metal ions occurring in brain in Parkinson's disease. J Neurochem 1989;52:1830–1836.
37. Sofic E, Riederer P, Heinsen H, et al. Increased iron (III) total iron content in post mortem substantia niga of parkinsonian brain. J Neural Transm 1988;74:199–205.
38. Good PF, Olanow CW, Perl DP. Neuromelanin-containing neurons of the substantia nigra accumulate iron aluminum in Parkinson's disease: a LAMMA study. Brain Res 1992;593:343–364
39. Griffiths PD, Dobson BR, Jones GR, Clarke DT. Iron in the basal ganglia in Parkinson's disease: an in vitro study using extended X-ray absorption fine structure cryo-electron microscopy. Brain 1999;122:667–673.
40. Antinoni A, Leenders KL, Meier D, Oertel WH, Boesiger P, Anliker M. T2 relaxation time in patients with Parkinson's disease. Neurology 1993;43:697–700.
41. Vymazal J, Righini A, Brooks RA, et al. T1 and T2 in the brain of healthy subjects, patients with Parkinson disease, patients with

multiple system atrophy: relation to iron content. Radiology 1999;211:489–495.
42. Ryvlin P, Broussolle E, Piollet H, Viallet F, Khalfallah Y, Chazot G. Magnetic resonance imaging evidence of decreased putamenal iron content in idiopathic Parkinson's disease. Arch Neurol 1995;52: 583–588
43. Chen JC, Hardy PA, Kucharczyk W, et al. MR of human postmortem brain tissue: correlative study between T2 assays of iron ferritin in Parkinson Huntington disease. AJNR Am J Neuroradiol 1993;14:275–281.
44. Bartzokis G, Aravagiri M, Oldendorf WH, Mintz J, Marder SR. Field dependent transverse relaxation rate increase may be a specific measure of tissue iron stores. Magn Reson Med 1993;29:459–464.
45. Bartzokis G, Cummings JL, Markham CH, et al. MRI evaluation of brain iron in earlier- later-onset Parkinson's disease normal subjects. Magn Reson Imaging 1999;17:213–222
46. Ordidge RJ, Gorell JM, Deniau JC, Knight RA, Helpern JA. Assessment of relative brain iron concentrations using T2-weighted T2*-weighted MRI at 3 Tesla. Magn Reson Med 1994;32:335–341.
47. Ye FQ, Martin WRW, Allen PS. Estimation of the brain iron in vivo by means of the interecho time dependence of image contrast. Magn Reson Med 1996;36:153–158.
48. Martin WRW, Ye FQ, Allen PS. Increasing striatal iron content associated with normal aging. Mov Disord 1998;13:281–286.
49. Ye FQ, Allen PS, Martin WRW. Basal ganglia iron content in Parkinson's disease measured with magnetic resonance. Mov Disord 1996;11:243–249.
50. Martin WRW, Roberts TE, Ye FQ, Allen PS. Increased basal ganglia iron in striatonigral degeneration: in vivo estimation with magnetic resonance. Can J Neurol Sci 1998;25:44–47.
51. Gorell JM, Ordidge RJ, Brown GG, Deniau, J-C, Buderer NM, Helpern JA. Increased iron-related MRI contrast in the substantia nigra in Parkinson's disease. Neurology 1995;45:1138–1143.
52. Graham JM, Paley MNJ, Grunewald RA, Hoggard N, Griffiths PD. Brain iron deposition in Parkinson's disease imaged using the PRIME magnetic resonance sequence. Brain 2000;123:2423–2431.
53. Vion-Dury J, Meyerhoff DJ, Cozzone PJ, Weiner MW. What might be the impact on neurology of the analysis of brain metabolism by in vivo magnetic resonance spectroscopy? J Neurol 1994;241:354–371.
54. Unrejak J, Williams SR, Gadian DG, Noble M. Proton nuclear magnetic resonance spectroscopy unambiguously identifies different neural cell types. J Neurosci 1993;13:981–989.
55. Matthews PM, Francis G, Antel J, Arnold DL. Proton magnetic resonance spectroscopy for metabolic characterisation of plaques in multiple sclerosis. Neurology 1991;41:1251–1256.
56. Chong WK, Sweeney B, Wilkinson ID, et al. Proton spectroscopy of the brain in HIV infection: correlation with clinical, immunologic MR imaging findings. Radiology 1993;188:119–124.
57. Shino A, Matsuda M, Morikawa S, Inubushi T, Akiguchi I, Handa J. Proton magnetic resonance spectroscopy with dementia. Surg Neurol 1993;39:143–147.
58. Gideon P, Henriksen O, Sperling B, et al. Early time course of N-acetylaspartate, creatine phosphocreatine, compounds containing choline in the brain after acute stroke. A proton magnetic resonance spectroscopy study. Stroke 1992;23:1566–1572.
59. Cwik V, Hanstock C, Allen PS, Martin WRW. Estimation of brainstem neuronal loss in amyotrophic lateral sclerosis with in vivo proton magnetic resonance spectroscopy. Neurology 1998;50: 72–77.
60. Christiansen P, Henriksen O, Stubgaard M, Gideon P, Larsson HBW. In vivo quantification of brain meabolites by 1H MRS using water as an internal standard. Magn Reson Imaging 1993;11:107–108.
61. Michaelis T, Merboldt KD, Bruhn H, Hanicke W, Frahm J. Absolute concentrations of metabolites in the adult human brain in vivo: quantification of localized proton MR spectra. Radiology 1993;187:219–227
62. Davie C. The role of spectroscopy in parkinsonism. Mov Disord 1998;13:2–4.
63. Clarke CE, Lowry M. Systematic review of proton magnetic resonance spectroscopy of the striatum in parkinsonian syndromes. Eur J Neurol 2001;8:573–577.
64. Holshauser BA, Komu M, Moller HE, et al. Localised proton NMR spectroscopy in the striatum of patients with idiopathic Parkinson's disease: a multicenter pilot study. Magn Reson Med 1995;33:589–594.
65. Davie CA, Wenning GK, Barker GJ, et al. Differentiation of multiple system atrophy from idiopathic Parkinson's disease using proton magnetic resonance spectroscopy. Ann Neurol 1995;37: 204–210.
66. Cruz CJ, Aminoff MJ, Meyerhoff DJ, Graham SH, Weiner MW. Proton MR spectroscopic imaging of the striatum in Parkinson's disease. Magn Reson Imaging 1997;15:619–624.
67. Tedeschi G, Litvan I, Bonavita S,. et al. Proton magnetic resonance spectroscopic imaging in progressive supranuclear palsy, Parkinson's disease corticobasal degeneration. Brain 1997;120: 1541–1552.
68. Clarke CE, Lowry M, Horsman A. Unchanged basal ganglia N-acetylaspartate glutamate in idiopathic Parkinson's disease measured by proton magnetic resonance spectroscopy. Mov Disord 1997;12:297–301.
69. Ellis CM, Lemmens G, Williams SCR, et al. Changes in putamen N-acetylaspartate choline ratios in untreated levodopa treated Parkinson's disease: a proton magnetic resonance spectroscopy study. Neurology 1997;49:438–444.
70. Clarke CE, Lowry M. Basal ganglia metabolite concentrations in idiopathic Parkinson's disease multiple system atrophy measured by proton magnetic resonance spectroscopy. Eur J Neurol 2000;7: 661–665.
71. O'Neill J, Schuff N, Marks WJ, Feiwell R, Aminoff MJ, Weiner MW. Quantitative 1H magnetic resonance spectroscopy MRI of Parkinson's disease. Mov Disord 2002;17:917–927.
72. Lucetti C, del Dotto P, Gambaccini G, et al. Proton magnetic resonance spectroscopy (1H-MRS) of motor cortex basal ganglia in de novo Parkinson's disease patients. Neurol Sci 2001;22:69–70.
73. Hu MT.M., Taylor-Robinson SD, Chaudhuri KR, et al. Evidence for cortical dysfunction in clinically nondemented patients with Parkinson's disease: a proton MR spectroscopy study. J Neurol Neurosurg Psychiatry 1999;67:20–26.
74. Federico F, Simone IL, Lucivero V, et al. Usefulness of proton magnetic resonance spectroscopy in differentiating parkinsonian syndromes. Italian J Neurol Sci 1999;20:223–229.
75. Axelson D, Bakken, IJ., Gribbestad IS, Ehrnholm B, Nilsen G, Aasly J. Applications of neural network analyses to in vivo 1H magnetic resonance spectroscopy of Parkinson disease patients. J Magn Reson Imaging 2002;16:13–20.
76. DiMauro S. Mitochondrial involvement in Parkinson's disease: the controversy continues. Neurology 1993;43:2170–2171.
77. Gu M, Cooper JM, Taanman JW, Schapira AHV. Mitochondrial DNA transmission of the mitochondrial defect in Parkinson's disease. Ann Neurol 1998;44:177–186.
78. Matthews PM, Allaire C, Shoubridge EA, Karpati G, Carpenter S, Arnold DL. In vivo muscle magnetic resonance spectroscopy in the clinical investigation of mitochondrial disease. Neurology 1991;41:114–120.
79. Penn AMW, Roberts T, Hodder J, Allen PS, Zhu G, Martin WRW. Generalized mitochondrial dysfunction in Parkinson's disease detected by magnetic resonance spectroscopy of muscle. Neurology 1995;45:2097–2099.
80. Barbiroli B, Martinelli P, Patuelli A, et al. Phosphorus magnetic resonance spectroscopy in multiple system atrophy Parkinson's disease. Mov Disord 1999;14:430–435.
81. Hu MTM, Taylor-Robinson SD, Chaudhuri KR, et al. Cortical dysfunction in non-demented Parkinson's disease patients. A combined 31P-MRS 18FDG-PET study. Brain 2000;123:340–352.
82. Jenkins BG, Koroshetz WJ, Beal MF, Rosen BR. Evidence for impairment of energy metabolism in vivo in Huntington's disease using localized 1H NMR spectroscopy. Neurology 1993;43:2689–2695.

83. Hoang TQ, Bluml S, Dubowitz DJ, et al. Quantitative proton-decoupled 31P MRS 1H MRS in the evaluation of Huntington's Parkinson's diseases. Neurology 1998;50:1033–1040.
84. Samuel M, Ceballos-Baumann AO, Blin J, et al. Evidence for lateral premotor parietal overactivity in Parkinson's disease during sequential biamanual movements. A PET study. Brain 1997;120:963–976.
85. Jahanshahi M, Jenkins, IH., Brown RG, Marsden CD, Passingham RE, Brooks DJ. Self-initiated versus externally triggered movements. I. An investigation using measurement of regional cerebral blood flow with PET movement-related potentials in normal Parkinson's disease subjects. Brain 1995;118:913–933.
86. Playford ED, Jenkins IH, Passingham RE, Nutt J, Frackowiak RS, Brooks DJ. Impaired mesial frontal putamen activation in Parkinson's disease: a positron emission tomography study. Ann Neurol 1992;32:151–161.
87. Sabatini U, Boulanouar K, Fabre N, et al. Cortical motor reorganization in akinetic patients with Parkinson's disease: a functional MRI study. Brain 2000;123:394–403.
88. Haslinger B, Erhard P, Kampfe N, et al. Event related functional magnetic resonance imaging in Parkinson's disease before after levodopa. Brain 2001;124:558–570.

2 Positron Emission Tomography and Single-Photon Emission Tomography in the Diagnosis of Parkinson's Disease

Differential Diagnosis From Parkinson-Like Degenerative Diseases

PAUL D. ACTON, PhD

SUMMARY

Parkinsonian symptoms are associated with a number of neurodegenerative disorders, such as Parkinson's disease, multiple system atrophy, and progressive supranuclear palsy. Positron emission tomography (PET) and single-photon emission tomography (SPECT) now are able to visualize and quantify changes in cerebral blood flow, glucose metabolism, and neurotransmitter function produced by parkinsonian disorders. Both PET and SPECT have become important tools in the differential diagnosis of these diseases and may have sufficient sensitivity to detect neuronal changes before the onset of clinical symptoms. Imaging is now being used to elucidate the genetic contribution to Parkinson's disease and in longitudinal studies to assess the efficacy and mode of action of neuroprotective drug and surgical treatments.

Key Words: Imaging; Parkinson's disease; multiple system atrophy; progressive supranuclear palsy; essential tremor; differential diagnosis; positron emission tomography (PET); single-photon emission tomography (SPECT); dopamine transporter; dopamine receptor; cerebral blood flow; cerebral glucose metabolism.

1. INTRODUCTION

The differential diagnosis of the various parkinsonian disorders based on clinical symptoms alone is difficult *(1–3)*. Clinical criteria for the diagnosis of Parkinson's disease (PD) provide high sensitivity for detecting parkinsonism but show poor specificity for identifying brainstem Lewy body disease or for differentiating atypical and typical PD *(4)*. Tremor is a classic feature of PD, although this can also be found in patients with progressive supranuclear palsy (PSP) and multiple system atrophy (MSA). Similarly, a general criterion for diagnosing PD is a good, sustained response to levodopa (L-dopa) therapy, although, again, this also is found in some patients with MSA and dopa-responsive dystonia. Indeed, some post mortem histopathological studies have shown that as many as 25% of all patients who were diagnosed with PD before death had been misdiagnosed *(1,2)*. Detecting preclinical disease by using biochemical markers for neurodegeneration has not been successful. Familial PD sometimes exhibits a mutation of the α-synuclein gene, but this cannot be used as a genetic marker for the majority of cases because the pathogenesis is rarely related to genetic mutation. These observations have contributed to the motivation for developing objective neuroimaging techniques that can differentiate between these disorders.

Structural changes induced by parkinsonian diseases are generally small and often only evident when the disease is in an advanced stage. Consequently, the diagnostic accuracy of anatomical imaging modalities (e.g., magnetic resonance imaging [MRI]) in neurodegenerative disorders is poor *(5)*. Preceding changes in brain morphology, alterations in the way the brain consumes glucose, or disruptions in regional cerebral blood flow (rCBF) may provide useful indicators of neurodegeneration. However, it is likely that changes in neurotransmitter function, most notably in the dopaminergic system, will become evident long before structural, metabolic, or blood flow variations.

In general, positron emission tomography (PET) and single-photon emission tomography (SPECT) imaging have provided a better platform for the diagnosis of parkinsonian disorders than MRI. Functional imaging of neurodegenerative disease with PET and SPECT has followed two main paths; studies of blood flow and cerebral metabolism to detect abnormal tissue functioning or imaging of the dopaminergic neurotransmitter system to study the loss of dopamine neurons.

2. IMAGING BLOOD FLOW AND METABOLISM

PET studies of cerebral glucose metabolism have used the glucose analog [^{18}F]fluorodeoxyglucose ([^{18}F]FDG), whereas radioactive water ($H_2{}^{15}O$), and the SPECT tracers ^{99m}Tc-hexamethylpropylene amine oxime (^{99m}Tc-HMPAO) and ^{99m}Tc-ethylcysteinate dimer (^{99m}Tc-ECD) are markers of cere-

From: *Bioimaging in Neurodegeneration*
Edited by P. A. Broderick, D. N. Rahni, and E. H. Kolodny

bral blood flow and perfusion. Striatal glucose metabolism and perfusion are generally found to be normal in PD *(6–10)*, although some studies have demonstrated an asymmetry of striatal metabolism *(11)*. Interestingly, atypical parkinsonian disorder has been differentiated from idiopathic PD by the appearance of striatal metabolic abnormalities in the atypical group *(12)*, which may provide a useful adjunct to routine clinical examination. Many studies have shown more global cortical hypometabolism or hypoperfusion or a loss of posterior parietal metabolism with a pattern similar to that observed in Alzheimer's, and other neurodegenerative diseases *(8,9,13–18)*. Others have used the differences in regional metabolism or rCBF to discriminate between PD and MSA *(10,19)* or PSP *(20)*. Studies of blood flow and glucose metabolism in patients with pure Lewy body disease with no features of Alzheimer's disease have consistently shown biparietal, bitemporal hypometabolism, a pattern that was once thought to represent the signature of Alzheimer's.

Imaging studies of glucose metabolism and CBF have shown important changes concomitant with degeneration in cognitive performance or autonomic failure *(21–25)*. Although blood flow studies have shown a poor correlation with laterality in hemi-Parkinson's patients *(26)*, there are clearly dramatic changes in CBF and glucose metabolism resulting from cognitive impairment *(18,27–29)*. This is similar in detail to patients with other neurodegenerative disorders, such as Alzheimer's disease and dementia with Lewy bodies *(30)*, but may be useful to distinguish vascular parkinsonism *(31)*. Interestingly, patients with gait disorders generally exhibit an internal verbal cue to compensate for the loss of control in the motor cortex *(32)*. Blood flow PET imaging also has been used to study the effects of novel therapies, such as Voice Treatment, on the reorganization of brain function to compensate for motor dysfunction *(33)*. Studies of blood flow and metabolism have indicated conflicting results when the on- and off-dopamine replacement therapy conditions are compared. Both reduced *(11,18,34)* and normal *(35,36)* regional glucose metabolism and rCBF have been reported after L-dopa treatment.

Recent advances in image analysis, using the voxel-based statistical techniques, such as statistical parametric mapping *(37,38)*, may provide greater accuracy in detecting focal changes in rCBF. These techniques compare changes in rCBF, voxel-by-voxel, or in glucose metabolism to identify regions of statistically significant differences. Although statistical parametric mapping has found important applications in studies of blood flow and metabolic changes in neurodegenerative disease *(39,40)*, it is limited to the comparison of groups of subjects, rather than the diagnosis of individuals. Other statistical methodologies have been developed to attempt to automate the diagnosis of patients with PD and other parkinsonian disorders, based on scans of individual subjects *(41,42)*.

3. IMAGING THE DOPAMINERGIC SYSTEM

In general, the diagnostic accuracy of CBF and glucose metabolism in differentiating neurodegenerative disorders is relatively poor in comparison with direct imaging of the dopaminergic nigrostriatal pathway *(20)*. Early PET studies of the nigrostriatal pathway used the uptake of 6-[^{18}F]fluoro-l-3,4-dihydroxyphenylalanine ([^{18}F]fluorodopa) as a measure of the integrity of dopamine neurons *(43,44)*. [^{18}F]fluorodopa measures changes in aromatic L-amino decarboxylase activity, which is dependent on the availability of striatal dopaminergic nerve terminals and is proportional to the number of dopamine neurons in the substantia nigra *(45)*.

Quantitative parameters associated with [^{18}F]fluorodopa uptake, such as the striatal-to-background uptake ratio, and the influx rate constant, have been shown to be useful indicators of dopaminergic degeneration in PD and other syndromes *(46–67)*. Indeed, [^{18}F]fluorodopa and PET are often regarded as the "gold standard" in the detection of dopamine neuronal loss *(68)*, although the contributions from SPECT imaging, and other direct measures of the dopaminergic binding sites, both pre- and postsynaptic, are increasing *(55,56,69–71)*. The analysis of [^{18}F]fluorodopa PET studies is known to have a number of serious potential problems. [^{18}F]fluorodopa is metabolized into a number of diffusible and nondiffusible labeled metabolites ([^{18}F]3-*O*-methyl-fluorodopa (3OMFD) in peripheral and brain tissue, and [^{18}F]dopamine (FDA), [^{18}F]3-4-dihydroxyphenylacetic acid (FdopaC), and [^{18}F]homovanillic acid in brain tissue). A further issue with the distribution of [^{18}F]fluorodopa in PET scans is the kinetic rate constants tend to disagree with in vitro measurements by a large factor (up to 10 times lower) *(72–76)*. Despite the fact that in vivo measurements of the decarboxylation rate, k_3, gave values considerably lower than in vitro measurements, it has been concluded that k_3 accurately reflects striatal aromatic L-amino decarboxylase activity in vivo with [^{18}F]fluorodopa PET *(75,76)*. Other technical considerations, which are common to all PET and SPECT imaging techniques, include partial volume effects *(62)*, which decrease the apparent striatal uptake of these tracers due to the limited resolution of the scanner.

Direct measurements of dopamine transporter binding sites are possible with [^{11}C]cocaine *(77)*, or the cocaine analogs 2β-carbomethoxy-3β-[4-iodophenyl] tropane (β-CIT) and *N*-ω-fluoropropyl-2β-carbomethoxy-3β-[4-iodophenyl] tropane (FP-CIT), labeled with either ^{18}F or ^{11}C for PET or ^{123}I for SPECT *(78–80)*. Other dopamine transporter ligands include *N*-[3-iodopropen-2-yl]-2β-carbomethoxy-3β-[4-chlorophenyl] tropane ([^{123}I]IPT) *(81)*, its 4-fluorophenyl analog [^{123}I]altropane *(82)*, 2β-carbomethoxy-3β-[4-fluorophenyl] tropane ([^{11}C]CFT) *(83)*, and [^{11}C]d-threo-methylphenidate *(84)*. Of particular importance is the recent development of the first successful ^{99m}Tc-labeled dopamine transporter ligand, ^{99m}Tc-Technetium[2-[[2-[[[3-(4-chlorophenyl)-8-methyl-8-azabicyclo[3.2.1] oct-2-yl]-methyl](2-mercaptoethyl) amino]-ethyl] amino] ethane-thiolato-*N*2,*N*2',*S*2,*S*2'] oxo-[1*R*-(exo-exo)] (^{99m}Tc-TRODAT-1) *(85, 86)*. Because ^{99m}Tc is so much more widely available and less expensive than ^{123}I, this new tracer could move imaging of the dopaminergic system from a research environment into routine clinical practice, particularly with simplified imaging protocols *(87)*.

Several tracers exist for imaging postsynaptic dopamine D2 receptors, using radioactively labeled dopamine receptor antagonists. The most widely used for SPECT include *S*-(-)-3-iodo-2-hydroxy-6-methoxy-*N*-[(1-ethyl-2-pyrrolidinyl) methyl] benzamide ([^{123}I]IBZM) *(88–90)*, *S*-5-iodo-7-*N*-[(1-ethyl-2-

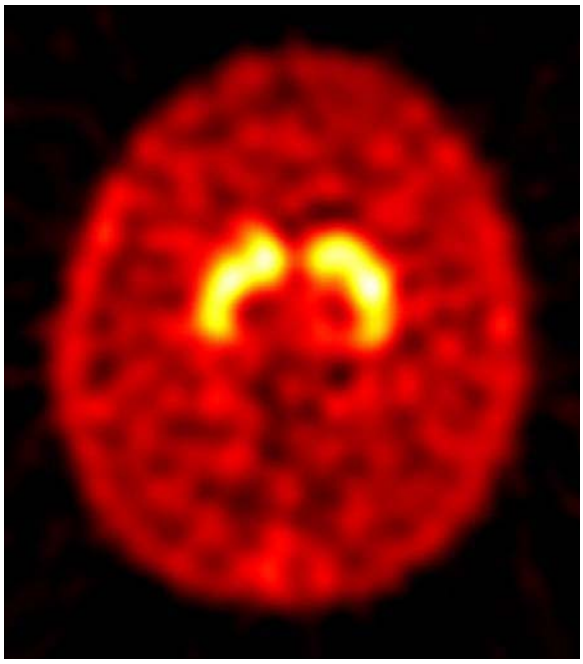

Fig. 1. Transaxial slice at the level of the striatum showing uptake of ^{99m}Tc-TRODAT-1 in dopamine transporters in a normal healthy volunteer. Good uptake is seen in the caudate nucleus and putamen, with background activity throughout the rest of the brain. Image courtesy of Dr. Andrew Newberg, University of Pennsylvania. *See* color version on Companion CD.

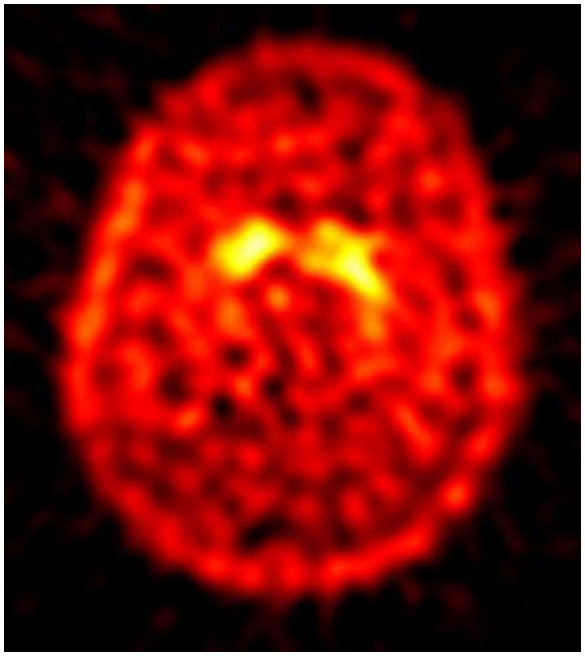

Fig. 2. Uptake of ^{99m}Tc-TRODAT-1 in the striatum of a patient with mild Parkinson's disease shows bilateral decrease in tracer concentration, particularly in the putamen, indicating a loss of dopaminergic neurons in these brain regions. Image courtesy of Dr. Andrew Newberg, University of Pennsylvania. *See* color version on Companion CD.

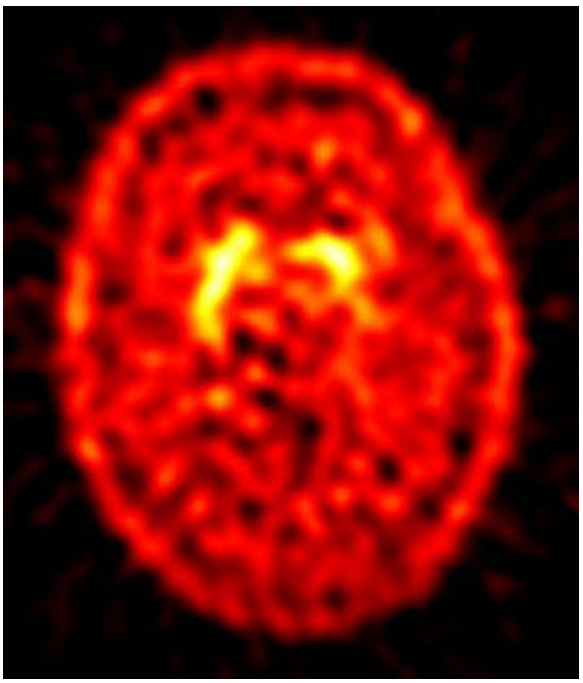

Fig. 3. A patient with hemi-PD exhibits a unilateral decrease in the uptake of ^{99m}Tc-TRODAT-1 in the side contralateral to clinical symptoms, most severely in the putamen. Although the clinical symptoms are confined to one side of the body, there also is reduced tracer uptake in the ipsilateral side, indicating a preclinical reduction in dopaminergic neurons, and demonstrating the sensitivity of imaging techniques for measuring dopaminergic dysfunction before clinical symptoms become apparent. Image courtesy of Dr. Andrew Newberg, University of Pennsylvania. *See* color version on Companion CD.

pyrrolidinyl) methyl] carboxamido-2,3-dihydrobenzofuran ([^{123}I]IBF) *(91,92)*, *S*-*N*-[(1-ethyl-2-pyrrolidinyl) methyl]-5-iodo-2,3-dimethoxybenzamide ([^{123}I]epidepride) *(93,94)* and for PET include *S*-(-)-3,5-dichloro-*N*-[(1-ethyl-2-pyrrolidinyl)] methyl-2-hydroxy-6-methoxybenzamide ([^{11}C]raclopride) *(95)* and [^{11}C] or [^{18}F]*N*-methylspiroperidol *(96,97)*.

PET and SPECT studies of radiotracer binding to postsynaptic dopamine receptors and presynaptic dopamine transporters have proved to be powerful techniques for quantifying the loss of dopaminergic neurons in normal aging *(98–107)*, PD *(67,108–162)* and other neurodegenerative disorders *(48, 143,163–184)*. Studies of neuronal degeneration associated with the effects of normal aging have indicated that, whereas dopamine transporter concentrations decrease as a natural consequence of aging, the changes are small compared with the effects of disease *(106)* (Fig. 1). PET and SPECT studies have indicated a consistent pattern of dopaminergic neuronal loss in PD, usually with more pronounced depletion in the putamen rather than in the caudate (Fig. 2). In addition, there is frequently a marked asymmetry, particularly in the early stages of the disease (Fig. 3), and a good correlation with symptom severity *(114,161)* and illness duration *(152)*. Most importantly, imaging studies may be sensitive enough to detect very early PD *(4,61,115,123,130,141,185–189)*, perhaps even before clinical symptoms become apparent.

Characteristically, PD begins with unilateral symptoms of motor deficit, which gradually progress bilaterally over time. Studies of patients with early hemi-PD have shown that, despite the subject exhibiting only one-sided clinical symptoms, the

PET and SPECT findings demonstrated bilateral decreases in tracer binding, with a greater reduction in the side contralateral to the clinical signs *(41,115,123,190,191)*. The ability of PET and SPECT to detect presymptomatic PD may have important consequences for the screening of familial PD *(187,188,192)*. PET and SPECT studies of parkinsonian kindreds have implicated a genetic foundation for familial PD, including mutations in the *parkin* gene. Hereditary parkinsonism has been detected in asymptomatic relatives with heterozygous *parkin* mutations, using imaging to determine the extent of neuronal damage *(187,193–196)*. Indeed, PET and SPECT imaging of the dopaminergic system is able to demonstrate presynaptic dysfunction in asymptomatic relatives, which is fully compatible with early parkinsonism *(187)*. Even subjects with apparently normal alleles exhibited reduced dopaminergic function on imaging, indicating a preclinical disease in these subjects that is likely to progress to full PD *(187)*. The same features were observed in asymptomatic twins, both monozygotic and dizygotic, of a sibling with parkinsonism *(188)*.

Although most of the PET and SPECT imaging studies have shown highly significant differences between groups of Parkinson's patients and age-matched normal controls, the statistically significant differential diagnosis of an individual subject is more problematic. Patients with severe PD are easily separated from healthy controls even by simple visual inspection of striatal images, quantified using some form of discriminant analysis *(122,126,150,152,164,186,197)*possessing a sensitivity and specificity close to 100% in the proper clinical setting. The differentiation between PD and vascular parkinsonism *(173,182)* and between PD and drug-induced parkinsonism *(133)* also appears possible using imaging of the dopaminergic system. However, patients presenting much earlier in the course of the disease are more difficult to detect, with potentially significant overlap with an age-matched control group *(185,198)* and consequential loss of diagnostic accuracy. The situation may be further complicated if the early differential diagnosis between several neurodegenerative disorders is required. Many of the symptoms associated with parkinsonian disorders are nonspecific, which is why the accurate clinical diagnosis of these diseases is difficult. Studies have shown little difference between radiotracer binding to dopamine transporters in patients with PD, MSA, or PSP *(164,166)* (Fig. 4). Based on current methods of analysis, it appears that the detection of early PD, or the differential diagnosis between various neurodegenerative disorders, may not be possible in individual cases based on imaging of a single neurotransmitter system alone *(121)*. Interestingly, progress on the differential diagnosis of PD and other parkinsonian disorders may come from PET and SPECT imaging outside the brain. Recent studies of the functional integrity of postganglionic cardiac sympathetic neurons, using [^{123}I]MIBG or [^{11}C]HED, have indicated a distinct difference between cardiac autonomic dysfunction in patients with PD and those with MSA *(199,200)*.

4. MULTIMODALITY AND MULTITRACER STUDIES

The relative merits of anatomical and functional imaging have been combined in some studies utilizing either several different radiotracers or data from both MRI/PET or SPECT. Regional glucose metabolism has been studied in parkinsonian disorders with [^{18}F]FDG and PET, and the data combined with striatal [^{18}F]fluorodopa uptake measurements to give an improved diagnostic indicator, and a better understanding of the underlying disease processes *(19,51,59,201)*. However, it should be noted that the improvement was relatively small over the good predictive capabilities of [^{18}F]fluorodopa by itself in these patient groups. Some studies have used the complementary information coming from structural MRI and functional [^{18}F]FDG PET in distinguishing between control subjects and patients with MSA *(53,202–205)*, in whom both focal MRI hypointensities, changes in striatal and midbrain size, and reduced glucose metabolism occurred on the side contralateral to clinical symptoms. Magnetic resonance spectroscopy adds an important new probe to complement functional PET and SPECT imaging studies *(204)*. Other studies have combined data from MRI and postsynaptic dopamine receptor concentrations using [^{123}I]IBZM and SPECT, giving useful information on the involvement of multiple brain regions in PSP *(206)* and MSA *(207)*.

However, the greatest discrimination between various neurodegenerative disorders may be found using PET or SPECT imaging of both pre- and postsynaptic dopaminergic function *(116,121,208)*. A study of [^{123}I]β-CIT and [^{123}I]IBZM binding in patients with early PD showed marked unilateral reductions in dopamine transporters measured by [^{123}I]β-CIT concomitant with elevated dopamine D2 receptor binding of [^{123}I]IBZM *(209)*. Recent SPECT studies investigating pre- and postsynaptic dopamine binding sites in the differential diagnosis of PD, MSA, and PSP have shown promising results, with a reduction in dopamine transporter availability in all diseases, and some discrimination between disorders in the pattern of dopamine D2 receptor concentrations *(142,210,211)* (Fig. 5). Similar results were observed in PET studies of early Parkinson's patients, where striatal [^{18}F]fluorodopa uptake was reduced and [^{11}C]raclopride binding was upregulated, with the degree of increase in dopamine receptor binding inversely proportional to disease severity *(47,53)*. These studies also used [^{18}F]FDG imaging of the same patients to determine the optimum combination of neuroreceptor function and glucose metabolism to differentiate between healthy controls and patients with PD *(47)* or MSA *(48,53)*. The results suggest that striatal [^{18}F]FDG and particularly [^{11}C]raclopride are sensitive to striatal function and may help with the characterization of patients with MSA, whereas [^{18}F]fluorodopa can accurately detect nigrostriatal dopaminergic abnormalities consistent with parkinsonian disorders. Other parkinsonian syndromes, such as Wilson disease, a disorder related to copper deposition, have been studied using imaging and demonstrate a significant decline in dopaminergic function, both pre- and postsynaptic, that can be differentiated from idiopathic PD *(170)*.

SPECT imaging of both pre- and postsynaptic dopamine binding sites simultaneously has now been performed in nonhuman primates, using ^{99m}Tc-TRODAT-1 and [^{123}I]IBZM or [^{123}I]IBF, separating the two radiotracers based on their different energy spectra *(212,213)*. The possibility of simultaneously imaging both dopamine transporters and D2 receptors in neurodegenerative disorders is an exciting prospect, providing a unique probe in the investigation and diagnosis of these diseases.

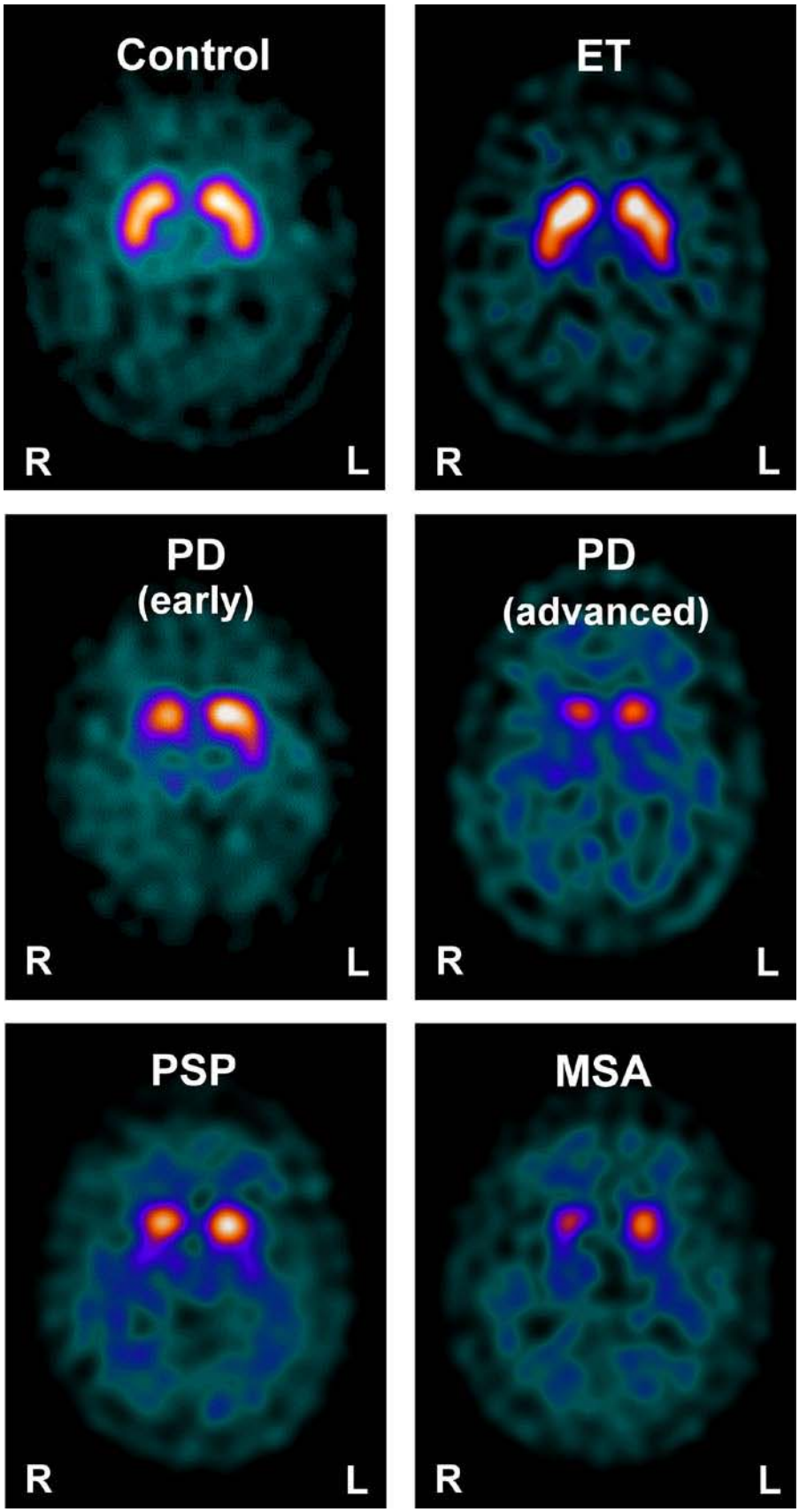

Fig. 4. Presynaptic dopamine transporter imaging with SPECT and [^{123}I]FP-CIT, used to distinguish between disease with and without nigrostriatal deficit. Whereas neurodegenerative parkinsonian syndromes such as PD, MSA, and PSP present with compromised dopamine terminal function, illnesses without involvement of those terminals (e.g., essential tremor [ET]) present with normal findings. Images courtesy of Prof. Klaus Tatsch, University of Munich. *See* color version on Companion CD.